



CAPE PENINSULA
UNIVERSITY OF TECHNOLOGY



Cape Peninsula University of Technology

Faculty of Engineering

Smart Structures and MEMS Lab

**Micromachined capacitive
accelerometer with crab-shape**

Fei Guo

B.Sc.Eng.(P.R.China)

Submitted towards the Master Degree of Technology
in Mechanical Engineering

Supervisor: **Prof. Dr. Bohua Sun**

Co-Supervisor: **Dr. Oscar Philander**

Cape Town, 2005

Acknowledgments

First of all, I must give special thank to my supervisor Prof. Dr. Bohua Sun who has always been a strong support through all these years of my graduate career and beyond.

Secondly, I need to thank my co-supervisor Dr. Oscar Philander and Mr. Keith Jacobs (HOD of Mechanical Engineering) for their kind consideration and help.

On the other hand, I shall thank the National Research Foundation (NRF) of South Africa and the Cape Peninsula University of Technology (CPUT) for their support on my research.

Finally, I would like to thank my mother and sister for giving financial support, considerate care and endearing encouragement to me during these two years.

Abstract

Perhaps more popular than the piezoresistive type are the capacitive type of micromachined accelerometers. The capacitive accelerometer has many fine characteristics, such as simple structure, high sensitivity, strong ability of resisting disturbance, fast dynamic response and so on. It can also work under abominable condition. So it is occupying an important status in the technology of electrical measurement and being used in many kinds of metrical systems.

In this paper, the capacitive accelerometer (CA) we will introduce and design is a parallel plate CA with crab-shape. It will detect the acceleration signal by the change of distance between two electrode plates, and its design standard came from the industrial requirements of KENTRON Company. The whole paper can be divided into four main phases—introduction, study, design and analysis.

At first, we have introduced the purpose and background of this thesis, and then the study and the discussion of relative literature. The content of these articles is mainly about the basic principle, types and applications of micro-sensors and this information will be very helpful to the design and analysis of my own CA.

The course of design is primarily structure design. The main structures of CA are parallel plate structure and cylinder structure. The parallel plate structure is chosen for our CA after we did the comparison of performance and technique of making between these two types of structures. We use the concentrative mass as the top electrode plate and four beams are connected on the two sides of the plate separately. The shape of plate has been optimized for meeting the design requirements. The final structure is a crab-shape structure. Its advantages are working stability, high sensitivity, high resonant frequency and low edge effect.

The analysis can be divided into three parts—analysis of vibration modes, mathematical analysis, parameter's analysis. We have used CoventorWare analyzing the vibration modes first. CoventorWare is software which can simulate and analyze micro-products. The purpose of this analysis is to get rid of the disturbance and effect of some unnecessary vibration modes. After the analysis to every mode, we adjust the relative area between two plates so as to these unnecessary modes cannot effect the change of capacitance. So we can only analyze the main vibration mode in after analysis.

Mathematical analysis includes the creation of math model, dynamic analysis, stress analysis and noise analysis. Math model is the relationship between the input value and output value. The main theorems we've used are capacitive concept, beam's analyzing theorem and Catigliano's theorem. We've also used Fourier series creating the linear equation between input and output value. In dynamic analysis, we've used a dummy structure for doing it and have created the dynamic formula of capacitance change. And then the maximum and minimum detectable acceleration has been found through stress analysis and noise analysis. According to those analyses and the requirements of KENTRON Company, we've then decided the measurements of this CA and have calculated some necessary parameters. The values of sensitivity and resonant frequency are high and they are also the advantages of our CA. The maximum and minimum detectable acceleration are much better than other types of CA so as to we can use it for more precise and veracious measurement.

At last, we've used the CoventorWare doing the parameters' analysis. This analysis mainly includes DC operation point analysis, DC transfer (sweep) analysis, Small signal AC analysis, Sensitivity analysis, Monte Carlo analysis, Impact of plate curvature, FEM analysis etc. Those analyses can show us the situation and distribution of these important parameters clearly. The Small signal AC analysis (resonant frequency analysis) shows that the relationship of frequencies between three axes (x, y, z) and there isn't obvious sympathetic vibration between them. The Impact

of plate curvature analysis shows us a curve which denotes a very little impact of plate curvature on our structure. These two points can prove that our CA's structure can work steadily.

Keywords: Capacitive accelerometer; Crab-shape; vibration mode; Sensitivity; Resonant frequency; MDS

摘要

Chinese Abstract

在现代传感器领域中,比压电式传感器更为流行的可能就是电容式传感器了。电容传感器在电子测量技术中占有十分重要的地位,广泛应用于各种测量系统。它具有结构简单,分辨率高,抗干扰能力强,动态响应快,能在恶劣工况条件下工作,并能实现非接触式测量等特点。而电容式传感器中的微加速度计无论在工业,军事等领域的应用就更加广泛。

本文设计和介绍的蟹脚形平行板电容加速度计主要是基于两平行板之间的距离变化,从而确定加速度的大小,其设计标准主要来源于 KENTRON 公司的工业要求。整篇论文主要包括介绍、学习、设计和分析等阶段。

最初,我们对整个研究的初衷、目标和背景作了一个大概的介绍,说明了设计和研究的目的与大环境。然后是对以前相关文章的学习和讨论,其中包括了微传感器的基本原理,类型和应用等。接下来的内容是整篇论文的核心,主要是对此电容式加速度计的设计和分析过程。

其设计主要是针对结构而言的。电容加速度计主要有平行板和圆柱形两种结构,将它们在性能及制作工艺上进行比较后,我们选用了平行板式结构,板采用集中质量,两端分别是两根末端固定的梁。为了达到设计要求我们还将可振动极板的形状进行了优化。最后整个结构为蟹脚形结构。它的优点主要在于其工作的稳定性和高频高灵敏度特性,并能一定量的减少边缘效应。

分析过程可分为三部分—模态分析,数学分析和工作情况模拟分析。在分析过程当中,我们使用了 CoventorWare 软件。此软件主要用于微机械和电子等产品的设计,模拟以及分析。结构选定以后,我们先对其进行了模态分析。分析目的是排除主模态以外其他模态的影响和干扰。对每个模态进行分析后,我们对下极板的面积加以调整,使其他模态无法对电容变化产生影响,以便我们在后面的数学分析中可以只对主模态进行分析。

数学分析包括数学模型的建立,动态分析,应力分析和噪音分析。数学模型即输入量(加速度)与输出量(电容变化)之间的关系式。此过程主要应用了电容理论和梁的分析理论以及能量法则—卡斯里亚诺法则 (*Castigliano's Theorem*)。我们还用傅立叶公式将其关系式线性化,建立了两值之间的线性公式。在动态分析中,我们使用了虚拟结构,并在最后建立了输出量(电容变化)的瞬时方程,其结果更说明了电容传感器动态响应快的特点。通过应力分析和噪音分析,我们找到了最大和最小测量加速度计算方程。根据以上分析和 KENTRON 公司的设计要求,我们接着设定了此加速度计的具体尺寸,并对一些重要参考参数进行了计算。灵敏度和响应频率的计算结果进一步证明了电容加速度计的高灵敏度和高频

特性，也说明了此加速度计的优势所在。另外，其最大和最小测量加速度的值远优于其他电容加速度计，这样使我们可以进行更精密和准确的加速度信号探测。在接着的工作情况模拟分析中，我们仍然使用 CoventorWare 软件。其分析主要包括：坐标点分析，电压随振动变化分析，最小信号分析（响应频率分析），灵敏度分析，蒙特卡罗分析（频率点分布分析），极板弯曲影响分析，有限元分析等。这些分析让人可以更直观地观察每个参数的状况及分布。其中响应频率分析显示了几个轴(x, y, z)之间的频率关系，几个轴之间无明显共振，极板弯曲影响分析的曲线表明了极板弯曲对此结构的影响很小，这两点也同时说明了此结构的工作稳定性。

在最后的结论和未来展望中，我们会对本电容加速度计的优势和不足做一定的讨论。

关键词：电容式加速度计；蟹脚形；模态；灵敏度；响应频率；最小测量信号

Table of Contents

Acknowledgments	I
Abstract	II
Chinese Abstract	V
Table of Contents	VII
List of Figures	XI
List of Tables	XIII
Chapter 1 Introduction	1
1-1. Motivation	1
1-2. Objectives	3
1-3. Background.....	4
1-3-1. (Micro) Sensors	4
1-3-2. The most familiar material for MEMS—silicon	5
1-3-3. Intro to capacitive accelerometer (CA)	6
1-3-4. Applications of CA.....	8
1-3-5. Development (history) of Accelerometer	9
1-4. Scope of thesis	12
Chapter 2 Literature Review	13
2-1. Micromechanical sensors principles.....	13
2-1-1. Basic structure of micromechanical	13
2-1-2. Sensing principles	14
2-2. Variety of micromechanical sensor	17
2-3. Accelerometers (acceleration sensors).....	18
2-3-1. The definition and applications of accelerometers.....	18
2-3-2. Some different types of accelerometers	20
2-3-3. Bandwidth and quality factor, Q, of accelerometers	21
2-4. Summary.....	21

Chapter 3 Structure Design and Analysis of Vibraton Mode	22
3-1. Introduction	22
3-2. Design of CA (Connolly, 1995).....	22
3-2-1. CA Element Design.....	22
3-2-2. CA package design	24
3-3. Introduction of some typical structure.....	25
3-3-1. Parallel plate CA	25
3-3-2. Cylinder CA	31
3-4. An example of CA (Garry et al, 2001).....	32
3-5. The analysis of these types of CA	34
3-6. Introduction of the structure of our CA	35
3-7. Analysis of vibration mode (simulated by CoventerWare).....	36
3-7-1. Process setting:.....	36
3-7-2. 2-D layout.....	37
3-7-3. Creation of mesh	38
3-7-4. Simulation of vibration modes	38
3-7-5. Analysis of six modes.....	42
3-8. Summary	43
Chapter 4 Establishment of Math Model and Mathematical Analysis	45
4-1. Introduction	45
4-2. Mechanics analysis of static model	45
4-2-1. Purpose of analysis.....	46
4-2-2. Analysis	46
4-2-3. Sensitivity	52
4-2-4. Resonant frequency	54
4-3. Dynamic analysis.....	55
4-3-1. dynamic mathematical model (Qing-Ming Wang, 2004)	55
4-3-2. Stress analysis	59
4-4. Noise analysis and establishment of measurement.....	61
4-4-1. Noise analysis (Gabrielson, 1993)	61

4-4-2. Minimum detectable signal (Oosterbroek, 1999).....	62
4-4-3. The establishment of measurement.....	63
4-5. Some necessary parameters' calculation.....	66
4-5-1. The formula of sensor.....	66
4-5-2. Sensitivity.....	67
4-5-3. The max detectable acceleration.....	67
4-5-4. The Brownian noise equivalent acceleration of the system.....	67
4-5-5. Thermal noise equivalent voltage spectral density (noise density).....	68
4-5-6. The bandwidth of the system.....	68
4-5-7. The minimum detectable signal.....	68
4-5-8. Elastic coefficient and resonant frequency.....	69
4-6. The introduction of circuit diagram of the accelerometer.....	70
4-6-1. The typical circuit sample of CA.....	70
4-6-2. The introduction of existing product's circuit.....	71
4-7. Summary.....	73
Chapter 5 Analysis by CoventorWare.....	75
5-1. Introduction of CoventorWare.....	75
5-2. Creation of architect model.....	77
5-3. Generate 2-D layout and 3-D model.....	79
5-4. Architect accelerometer performance analysis.....	80
5-4-1. DC operation point analysis.....	80
5-4-2. DC transfer (sweep) analysis.....	81
5-4-3. Small signal AC analysis.....	82
5-4-4. Sensitivity analysis.....	83
5-4-5. Monte Carlo analysis.....	85
5-4-6. Impact of plate curvature.....	85
5-4-7. FEM analysis.....	88
5-5. Summary to the result of analysis.....	88
Chapter 6 Conclusions and Recommendations.....	90
6-1. Summary.....	90

6-2. Conclusion.....	91
6-3. Recommendations for the future	92

References

Resume of Fei GUO

List of Figures

- Figure (1-1):** Typical Capacitor Transducer Conditioning Circuit
- Figure (1-2):** Principal sketch of MEMS
- Figure (1-3):** Abridged layout of servo type MEMS accelerometer
- Figure (2-1):** Various ways of connecting a beam to its surroundings: a), b), c), d)
- Figure (2-2):** Two examples of (circular) membranes. Left, Right
- Figure (2-3):** Example of a micro-bridge resonator for flow-measurements
- Figure (2-4):** Simplified lumped element representation of an accelerometer
- Figure (3-1):** The beams in the suspension system supporting the inertial mass are typically 9 microns wide and 1.5 microns thick
- Figure (3-2):** The Model 7594 OEM accelerometer is 5/8 by 5/8 in. with a height of 0.15 in. The weight is 1.6 g. The cover has been removed to display the sensor element and conditioning circuitry
- Figure (3-3):** structure of parallel CA with style of distance change
- Figure (3-4):** the curve of characteristic of $C=f(\delta)$
- Figure (3-5):** structure of parallel CA with style of area change
- Figure (3-6):** structure of teeth-shape
- Figure (3-7):** structure of parallel CA with style of dielectric change
- Figure (3-8):** coaxial cylinder CA
- Figure (3-9):** Topology design and wiring configuration of the z-axis accelerometer
- Figure (3-10):** principle of z-displacement capacitive-sensing through comb-finger
- Figure (3-11):** capacitive accelerometer with crab-shape structure
- Figure (3-12):** the design of process of MEMS
- Figure (3-13):** the 2-D layout of the structure
- Figure (3-14):** the mesh mode of the structure
- Figure (3-15):** The 1st vibration mode of the structure
- Figure (3-16):** the graph of capacitive change of first mode

- Figure (3-17):** The 2nd vibration mode
- Figure (3-18):** The 3rd vibration mode
- Figure (3-19):** The 4th vibration mode
- Figure (3-20):** The 5th vibration mode
- Figure (3-21):** The 6th vibration mode
- Figure (3-22):** the relative change of distance
- Figure (4-1):** Separate it into two parts
- Figure (4-2):** Status of force and bending moment act on the beam
- Figure (4-3):** The deformation of the beam
- Figure (4-4):** Sensitivity 35,000 Ohms/K @ 4.2 K
- Figure (4-5):** the sketch map of difference configuration
- Figure (4-6):** Dynamic model of accelerometer
- Figure (4-7):** Measurement of structure
- Figure (4-8):** A typical circuit diagram for capacitive accelerometers
- Figure (4-9):** Photo of Silicon Microstructures' 7130 Capacitive Micro machined Accelerometer
- Figure (4-10):** The two axes sensor
- Figure (4-11):** The one axis sensor
- Figure (5-1):** the flow map of CoventorWare working
- Figure (5-2):** the block diagram of architect work
- Figure (5-3):** the architect model of our accelerometer
- Figure (5-4):** 2-D layout generated by architect model
- Figure (5-5):** 3-D model
- Figure (5-6):** DC transfer (sweep) analysis
- Figure (5-7):** the resonant frequencies of three axes
- Figure (5-8):** resonant frequencies of varying beam length
- Figure (5-9):** result of Monte Carlo analysis
- Figure (5-10):** result of vary analysis
- Figure (5-11):** 3-D mesh mode for doing FEM analysis

List of Tables

Table (2-1): Specifications of accelerometers for three applications

Table (3-1): The characteristics of Differential CA with comb-fingers

Table (3-2): frequencies in six modeDomains

Table (4-1): Part of characters of silicon

Table (4-2): Guideline of performance of analog products

Table (4-3): Measurements of structure

Table (4-4): the important parameters of our CA

Table (5-1): coordinate values for X, Y and Z axes

Table (5-2): sensitivity report

Table (5-3): operating point report of plate curvature

Table (5-4): frequency results

Table (6-1): comparison of parameters

Chapter 1

Introduction

1-1. Motivation

In modern society, the requirement for industrial technology is increasing rapidly along with the improvement of science property and the boost of level of people's living. Thus the demand for new generations of many fields, such as industrial, military, commercial, medical, automotive and aerospace products have been a strong driving force behind the research and development of sensors. This situation has been further stimulated by the intellectual curiosity of humankind. Global competition among the principal industrial nations has also been a parameter in the equation is governing the rate of technological progress.

Under the influence of the micromation current of the product designing, micro-sensors are concerned and applied in the industrial more and more. By integrating the knowledge-base associated with advanced materials, information technology and integrate circuit, these three mega-technologies are facilitating the creation of a new generation of micro-electro-mechanical systems (MEMS). This technology has impacted and will bring more revolution on our lifestyles in the future.

For high resonant frequency, micro sensor can be applied in many different fields, such as high-resolution positioning, high strike and tiny mass detection.

During the last decade, lots of investigations have been done on the micro-sensor field. For instance, Arjun Selvakumar, Farrokh Ayazi and Khalil Najafi (1996) designed a z-axis capacitive accelerometer with large sensitivity. Chingwen. Yeh and

Khalil Najafi (1995) created a low-voltage tunneling-based silicon microaccelerometer, which is fabricated using bulk silicon micromachining technology and the boron etch-stop dissolved wafer process. Timo Veijola, Heikki Kuisma and Juha Lahdenpera (1999) researched the possibility of large-displacement capacitive accelerometer. Navid Yazdi, Farrokh Ayazi and Khalil Najafi (1998) presented a review of silicon micromachined accelerometers. Y. Nemirovsky, A. Nemirovsky, P. Muralt and N. SetterPZT (1996) focused on the design of thin film piezoelectric accelerometer. H.G. Yu, L. Zou, K. Deng, R. Wolf, S. Tadigadapa and S. Trolier-McKinstry (2003) discussed the piezoelectric thin film accelerometer manufacture. A. Spineanu, P. Benabes and R. Kielbasa (1997) researched the measurements of piezoelectric thin film accelerometer. D. Eicher, M. Giousouf and W. von Munch (1999) analyzed vibration and electromechanical sensitivity of micro-sensor with four piezoelectric thin films. L. Ries and W. Smith (1999) analyzed various arrangements of deformable sensors using the finite element theory. J. Yu and C. Lan (2001) introduced the design of thin film piezoelectric accelerometer; Qing-Ming Wang, Zhaochun Yang, Fang Li and Patrick Smolinski (2004) has done analysis on a “+” shape beam with four piezoelectric thin films elastic characteristics of the thin films.

There are also some companies and enterprises in which the micro-sensors and actuators technique has been developing for many years. The most typical example is the company by the name of “analog” which is producing professional micro industrial production. 15 years ago, Analog Devices revolutionized automotive airbag systems with its unique *iMEMS*® (integrated Micro Electro Mechanical System) accelerometers. *iMEMS* accelerometers were the first products in an array of Motion Signal Processing™ solutions to use innovative design techniques to integrate small, robust sensors with advanced signal conditioning circuitry on a single chip. Today, ADI offers the industry's broadest accelerometer portfolio, with products addressing a range of user needs including high performance, low power consumption, and small size. The ADXL products are the foundation for Analog Devices' accelerometer family, and utilize the *iMEMS* surface micromachining process that has been used to ship

over 200 million sensors for automotive safety, consumer and industrial applications. This technology enables volume production of reliable, high quality, cost-effective products. Available in low-g or high-g sensing ranges, *i*MEMS accelerometers are used to measure position, motion, tilt, shock, and vibration in a broad array of applications. Further information about the analog can be obtained from its website (the Product of Analog)

But the number of the company like analog who has comparatively large scale and authoritative technique is still few. Therefore the technician who is working in this field is still very scarce. And the skill of designing and manufacturing of micro sensor and actuator still needs to improve and develop.

In this paper, our work will concentrate on designing of a simpler structure sensor, a crab shape sensor, than before. In particular, we focus on capacitive accelerometer. The main parameters of this kind of accelerometers were studied. Many kinds of analysis for the model and numerical simulations of it will be done all by using CoventorWare 2004—a special software for simulating and analyzing micro product. The results will give out the rules for designing.

1-2. Objectives

The main purpose of the work is to obtain some useful and practical rules of the capacitive accelerometers with crab-shape, and then attain the objective that accomplishes a better structure than former existing productions, and let this new configuration sensor can work in a higher level. Supporting tasks, which highlight the major contributions of this thesis, are the following:

- Design a practical structure for this capacitive accelerometer which is also convenient for making

- Develop its working performance and capability on the basis of reducing cost and clarify pivotal definitions and issues within the whole course of design
- Simulate the working situation and analyze the characters of this crab-shape accelerometer to verify its capability

The last aim will be to give some references for the design of micro accelerometers. For industrial field, the major objective is to provide a possibility of the product manufacturing process and application.

1-3. Background

1-3-1. (Micro) Sensors

A sensor, a transducer, transmitter and detector or often used as synonyms. They are devices that convert one form of energy into another and provide the user with a usable energy output in response to a specific measurable input.

The field of sensor which is relatively new but has already filled bookshelves with meters of journal and conference papers and which has attracted great activity in the past 10-15 years.

The modern technical world demands the availability of sensors to measure and convert a variety of physical quantities into electrical signals. These signals can then be fed into data processing systems and electronically evaluated and processed. Sensors can therefore be regarded as links between the nonelectrical environment and dataprocessing electronic systems.

There is an important system aspect of microsensors: being small, and generally producing small signals, they do not trivially interface with the macro-world.

Therefore, micromechanical sensors cannot be viewed as separate entities but they should actually be considered as *microsystems* involving not only the sensing microstructure but the interfacing and packaging as well. Hence, the design and development-process of microsensors should simultaneously include the interfacing and packaging aspects in order to successfully come to a working *micro-sensor-system*. In some cases, where one cannot rely on standard technology (i.e. in the form of foundry-processes), it may be even necessary to design the microfabrication processes hand in hand with the microsystems.

The foregoing also reveals the multi-disciplinary nature of microsensorsystems; not only are the mechanical properties of structures important, but generally all the physical domains that take part in the transduction of the measurand to the eventual signal. This may involve such things as mechanics, for the actual response of the sensor (i.e. a bending membrane), optics (for read-out of a displacement), opto-electronic conversion and electronics for further signal processing. Moreover, the sensorsystem needs to be packaged. Although packaging of electronic integrated circuits is not a trivial thing, packaging a microsensor may even be more challenging by the very sole reason that a sensor should somehow "be open" to the environment in order to measure the measurand. This means, that apart from an electrical interconnection, it needs at least one other physical connection. Also from this point of view, the design and development of microsensorsystems requires multidisciplinary teams and system approaches, rather than sole monodisciplinary depth.

1-3-2. The most familiar material for MEMS—silicon

Although the term MEMS is not restricted to *silicon* micromachining, most of today's MEMS technology is based on silicon. This is, off course, for good reasons. Silicon mono-crystalline wafers offer a good combination of qualities, ranging from ideally elastic (no creeps or hysteresis) to a good heat conductor, from low to intermediate

electrical conductivity (depending on type and doping), from having a small thermal expansion coefficient to being stable up to high temperatures. (Petersen, 1982) More importantly, silicon wafers are produced and used on a large scale for integrated microelectronics resulting in low prices and compatible equipment. Additionally (with certain restrictions on technology) silicon wafers allow for monolithic integration of mechanical and electronic functions in one and the same chip offering a high potential for both cheap and advanced sensor systems. Therefore, the majority of MEMS devices are made on silicon wafers as the starting substrate.

1-3-3. Intro to capacitive accelerometer (CA)

Capacitive sensors are generally used for linear rather than angular proximity measurement. Either the dielectric or one of the capacitor plates is movable for angular or linear displacement measurement. Capacitive proximity sensors use the measured object as one plate, while the sensor contains the other plate. The capacitance changes as a function of the area of the plates, the dielectric, or the distance between the plates. Capacitive transducers are available with packaged signal conversion circuitry for DC output operation. Accuracy for small displacements can be near the order of 0.25%, with accuracies of up to 0.05% available at a higher cost.

Capacitive devices are accurate, relatively small devices with excellent frequency response. Their greatest weakness is probably their sensitivity to temperature or the need for additional electronics to produce a usable output. A typical capacitor transducer circuit is shown in Figure (1-1). An AC voltage is applied across the plates to detect changes. The capacitor can also be made part of an oscillator circuit causing an output frequency to vary.

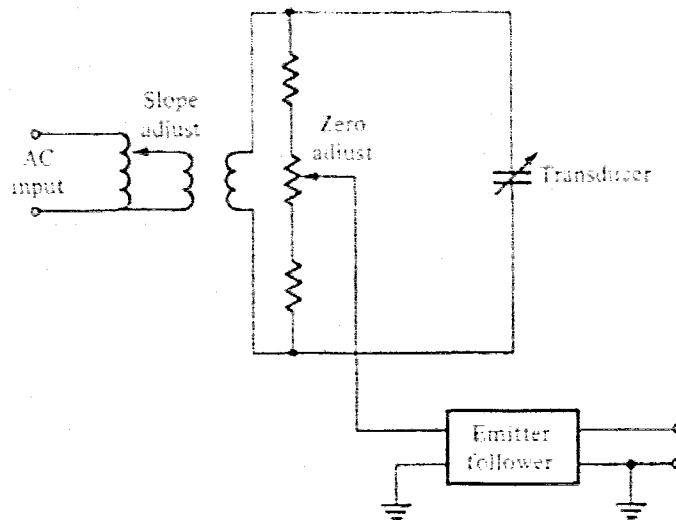


Figure (1-1): Typical Capacitor Transducer Conditioning Circuit

These devices have good linearity and good output resolution. Disadvantages are the temperature and cable sensitivity which require the amplification circuitry to be located close to the transducer. For more information about capacitive accelerometers, please check the website (Pc-control)

Capacitive acceleration transducers use a change of capacitance in response to acceleration. Some transducer designs use a fixed stator plate and a diaphragm to which a disc shaped seismic mass is attached. The diaphragm acts as the restraining spring as well as the moving electrode of the capacitor. Acceleration acting on the mass causes the diaphragm to deflect and its capacitance to the stator to change proportionally. Those knowledge can be learnt from the web page (Schwingungsmesstechnik)

The capacitive transduction principle is employed in some accelerometer designs, which typically use a diaphragm-supported seismic mass or a flexure-supported disk-shaped seismic mass as the moving electrode and either one or two fixed electrodes (stator plates). As acceleration is applied, the proximity between moving and fixed electrodes changes. This results in a change of capacitance, a simple

capacitance variation if one stator plate is used, and a differential change in two capacitances if the moving electrode is located between two stator plates. Various signal-conditioning schemes have been applied to such transduction elements. The element can be connected into an AC bridge and a change in transducer AC output voltage (or DC output, if the signal is rectified) occurs. The element can be connected as the capacitor in the LC or RC portion of an oscillator circuit so that a change in transducer output frequency results in response to changes in applied acceleration. The capacitance changes in a two-stator transduction element have also been used in a switching circuit so that a pulse train is generated in which pulse width and distance between pulses are the result of the changes in the two capacitances. Single-stator elements have been used in some servo accelerometers. An experimental triaxial accelerometer design uses a freely moving spherical metallic mass and three stator elements arranged in three mutually orthogonal axes, in a spherical evacuated cavity containing the mass, to provide outputs in the form of capacitance changes for acceleration along any axis. This design, sometimes called “drag free” can also be furnished with a set of three torquer coils and can then operate in a closed-loop servo mode.

1-3-4. Applications of CA

In modern society, the capacitive accelerometer has already been used in many different fields. CA is operating very important function in industry, military, aviation, seafaring, etc.

- Gun-Launched Projectile Guidance
- Missile Guidance and Flight Control
- Missile Safe-and-Arm
- Aircraft Flight Test

- Launch Vehicle Load

1-3-5. Development (history) of Accelerometer

The first accelerometer, originally known as the Atwood machine, was invented by the English physicist George Atwood (1746-1807) in 1783. There are two types of accelerometers. The instrument constructed by Atwood measures linear acceleration ($F=ma$), such as that experienced by a falling object. A spring system is used to measure the accelerating force, which provides the acceleration via Newton's famous second law, force equals mass times acceleration. Later accelerometers were designed to measure circular or twisting acceleration, such as that experienced by a weight spun at the end of a string. Here the acceleration depends on the radius of the circle of the spinning object (Bookrags- Accelerometer).

There was little need for the Atwood accelerometer until the rise of the automobile industry. As demand increased, automakers found it necessary to make their vehicles safer and more efficient. By placing many accelerometers in a test vehicle, researchers are able to determine where the engine's power is being dispersed. Simple forward acceleration can be measured, of course, but so can the sideways and up-and-down shift within the car's frame. Automotive researchers often place a human-sized dummy containing several accelerometers inside a moving vehicle in order to determine the effect of the car's motion upon a passenger, which information can be accessed via the web pages (Bookrags- Accelerometer)

The rapid development of semiconductor manufacturing technologies enabled development and mass manufacturing of various sensors and actuators using state of the art technologies. Devices, whose operation principle is based on use of miniature mechanical elements, are denoted as Micro Electro-Mechanical Systems (MEMS). Also in the field of vibration measurement such systems have been developed and are marketed (Hutyra, 1994 and Doescher, 1999 and Stein, 1995a and Stein, 1995b).

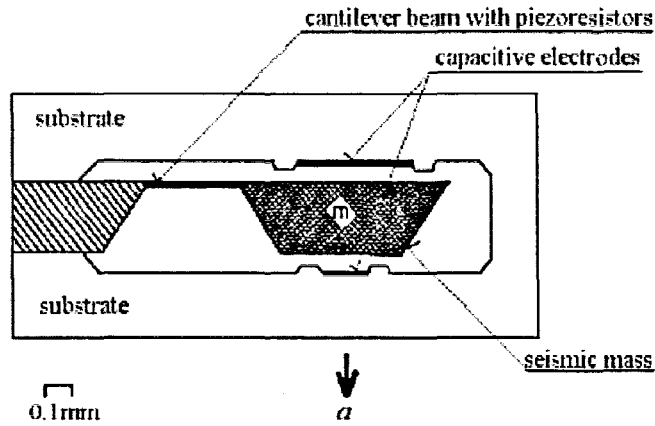


Figure (1-2): Principal sketch of MEMS.

The above physical principles and methods of transducing of mechanical variables into electrical ones are used (Berter, 1993 and Bernstein et al, 1999). The principal sketch of MEMS type sensor is in Figure (1-3), where also the first two mechano-electrical transducing principles are indicated.

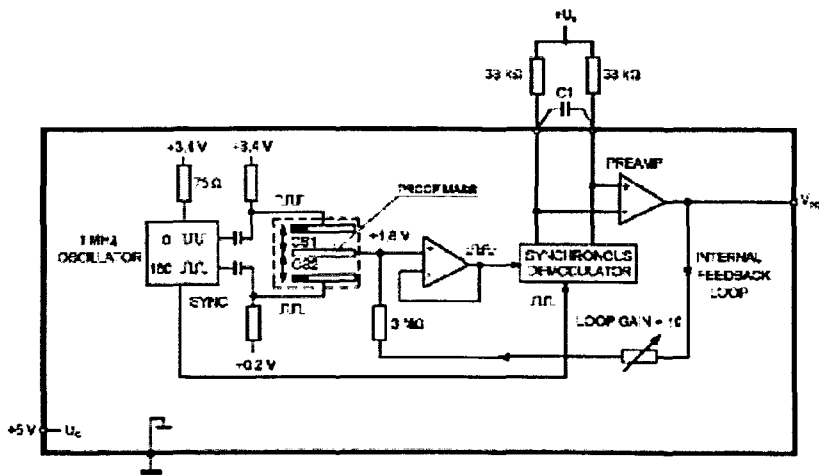


Figure (1-3): Abridged layout of servo type MEMS accelerometer (after (Stein, 1995a)).

Differential capacitor principle is often used in commercial applications (Hutyra, 1994 and Doescher, 1999); the servo-accelerometer principle is used widely too (Doescher, 1999 and Stein, 1995a) (Figure (1-3)).

The servo-accelerometer principle is following (Stein, 1995a): the sensitive element (dashed) is a comblike structure of 46 differential capacitors arranged in parallel on a beam forming the seismic mass supported by springs etched from silicon substrate. The differential capacitor forms a capacitive half-bridge driven from a high frequency square wave generator by opposite phase pulses. When acceleration is applied perpendicularly to the seismic mass the differential capacitor is mismatched and a non-zero signal appears on the central plate. This signal is preamplified, demodulated in the synchronous detector, amplified and outputted as voltage V_{PR} , corresponding to the applied acceleration. The demodulated signal V_{PR} is feedback via the internal loop 3 M Ω resistor to the differential capacitor's central plate, so providing the electrostatic restoring force to move the beam to the original centred position. Further signal processing is provided on-board by a build-in signal conditioning/band-limiting amplifier. Further improvements (Stein, 1995b) consist of addition of a temperature sensor to compensate for temperature influence and of using an on-board voltage-to-duty cycle converter to improve connectivity to micro-controller (no ADC is required; instead counter inputs are used).

Accelerometers are gaining ground in many military and aerospace applications thanks to reductions in price and size, greater operating ranges, higher resonant frequencies, lower amplitude ranges, MEMS technology, and integral electronics, but several challenges remain.

A review of trends in accelerometer design intended to support the military and aerospace industry reveals a number of interesting developments in cost, size, frequency response, range, reliability, and integral electronics. Decreases in cost have resulted in increased use of accelerometers for control and monitoring. Size reductions continue to minimize mass loading of structures, while some increase in range is enhancing the pyroshock testing of aerospace components. Higher resonant frequencies are helping improve accelerometer survivability in pyroshock environments. Lower amplitude range and frequency response capabilities are

enhancing the modal testing of large aerospace structures. MEMS sensor technology and the incorporation of electronics into the accelerometer housing are enhancing reliability. Smart accelerometers offer additional promise to the military and aerospace industry. Further information about the development of accelerometers can be obtained from website (Sensorsmag)

1-4. Scope of thesis

There are six chapters in this thesis. Chapter 1 is the introduction of micro sensors and the capacitive accelerometer. The development and applications in many fields of accelerometer will also be discussed. There will be the literature review in Chapter 2. Some relative articles and products will be introduced and analyzed. They are mainly about microsensor, accelerometer, etc. Chapter 3 will be the design of structure of my capacitive accelerometer and analysis of vibration form, in which the first and main vibration mode will be determined. Next, the core part of whole paper—mathematical and CoventorWare analysis will be done in chapter 4 and chapter 5. The math model will be created and some important parameters will be calculated in chapter 4. After that, we will use MEMS software—CoventorWare analyzing our capacitive sensor. The last Chapter 6 will be conclusion and recommendation for future. We'll compare the capabilities of our CA with existing products and find an easier way to making MEMS sensor.

Chapter 2

Literature Review

2-1. Micromechanical sensors principles

2-1-1. Basic structure of micromechanical

Micromechanical sensors, as the name suggest, contain some mechanical structure of which certain properties depend on specific (physical) environmental conditions. In general one can say that the mechanical structure is deformed in some way. How this deformation is sensed and turned into a (electrical) signal is a second question.

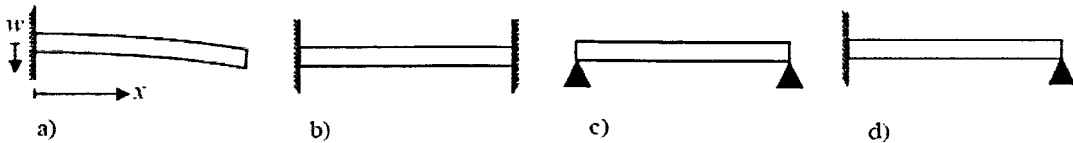


Figure (2-1): Various ways of connecting a beam to its surroundings: a) clamped-free (cantilever beam) b) clamped-clamped (bridge) c) simply supported-simply supported d) clamped-simply supported.

The way mechanical structures deform, not only depends on their shapes but also on the mechanical properties (Young's modulus E , Poisson ratio ν , mechanical load (stress-)distribution $\sigma(x, y, z)$, the way they are connected to their surroundings and, hopefully, some environmental (physical) parameter(s), e.g. pressure, temperature, humidity, acceleration, rotation etc. Examples of mechanical members are beams (one/two side clamped, free-hanging, etc.), membranes, diaphragms, mass-suspension systems (e.g. for acceleration sensing).

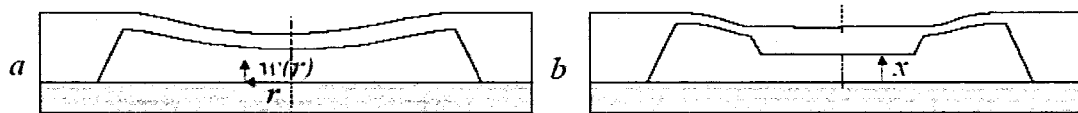


Figure (2-2): Two examples of (circular) membranes.
Left: simple diaphragm. Right: centrally strengthened diaphragm (boss).

Apart from static deformations mechanical changes can be well observed in dynamic behavior. As an example we mention the influence of stress on the resonance frequency of micro-bridges. On increasing the stress the resonance frequency will increase as well, an effect well-known from e.g. macroscopic string-instruments. Resonant sensors can achieve very high resolutions of 100 ppm or better.

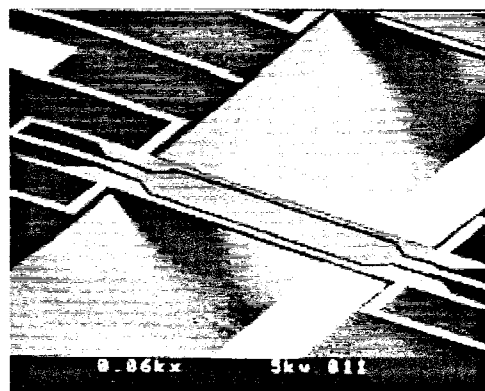


Figure (2-3): Example of a micro-bridge resonator for flow-measurements

2-1-2. Sensing principles

Once a mechanical structure shows a static or dynamic change, there are several ways of sensing these changes. Depending on the technologies used and the scale of the mechanical effects one or the other method may be favorable. One of the sensing principles best known from macroscopic mechanical structures is the strain gauge. The electrical resistance of a piece of metal depends on its size and shape. For a rod with cross-section S and length l the resistance R is given by $R = \frac{l}{\lambda S}$ with λ the

specific conductivity. If as a consequence of an external load the resistor changes its dimensions the resistance will change due to both a change in length and in cross-section. The relative change of the resistance is given by Wiegerink and Elwenspoek (2000): $\frac{dR}{R} = (1 + 2\nu)\epsilon$ where ν is the Poisson ratio. The ratio of the relative change of the resistance per unit strain is called the gauge factor G . Typical values of ν are 0.1 - 0.4, so for most materials the gage factor is between 1 and 2. The yield strain of metals mostly is well below 1% (this is about the yield strain of high quality steel) so changes in resistance of metal strain-gauges is at maximum 1 to 2%. Metal strain gauges are very well developed. There are commercial strain-gauges of all possible kinds, including temperature compensated strain-gauges, and including strain-gauges matching a great number of materials (with respect to thermal expansion coefficient). As an indication there are loadcells based on metal strain-gauges with a precision of 1:100,000, guaranteed in a temperature range between -40 and +80 °C (outperforming current sensors made by micro-machining). The dominant effect in metal strain-gauges is the change of the geometry; the materials property λ is independent of the strain. This is different in semiconductors. Here the effect is called piezo-resistivity. Conductivity, and therefore all effects connected to conductivity such as piezo-resistivity in crystals are anisotropic (Kloek et al 1994). The piezoresistive coefficient π is defined as the relative change of the resistivity per unit of stress. There is a longitudinal and a transversal effect: the resistivity changes in a direction parallel to the strain and normal to the strain. The effect is observed in single crystalline MESA+ Micromechanical Sensors GK 9 silicon as well as in polysilicon thin films. In single crystalline silicon the effect is exploited by doping p-regions in n-type silicon microstructures. Polysilicon thin films can be deposited on top of microstructures, doped and patterned. The gauge-factor for p-doped <110> Si is 133, much larger than the geometrical effects (Wiegerink et al, 1999).

A second method for deformation (displacement-) sensing is using electrostatics.

Basically when two electrically conducting bodies are put in each others neighbourhood they form a capacitor. Changing the geometry this capacitance will change as well. This change can either be detected by a variation in voltage (e.g. when using "frozen electrical charges" as in the case of electret microphones) or by the change in capacitance (e.g. by incorporating the structure in an oscillator circuit such that the oscillation frequency becomes a measure for the position of the two bodies relative to each other (Wiegerink et al, 1999).

Yet other sensing is based on temperature and heat conduction effects. Various principles are possible. E.g. when two plates are positioned relatively close to each other, the heat transfer through the medium filling the gap in between the plates is largely influenced by the pressure of the medium only saturating at pressures for which the mean free-path becomes smaller than the gap (Burger et al, 1998). Other quantities may be sensed indirectly by determining the temperatures. This is for example the case for flow-sensors where the cooling of a wire (-like) structure by a passing flow is a measure for the magnitude of the flow (anemometry). Temperature (-differences) can be well measured by the temperature resistance effect, for example by using platinum wires (Wiegerink et al, 1999).

Many sensing principles are based on geometrical changes. However, when using piezo-electric materials, the transduction takes place inside the material. Applying a stress over a film of piezoelectric material directly results in a voltage-drop over the thickness (and width) of the layer. Although piezo-electric transduction is often used in macroscopic sensors and actuators, it is less often found in micro-mechanical transducers the reason being a lack of materials which can be deposited with sufficient quality and durability (e.g. zinc-oxide suffers from charge injection whereas materials like PZT are more difficult to apply in thick films).

In many cases it may be advantageous to have no electrical in- and output signals to a sensor, e.g. when operating in environments with a large level of electromagnetic

radiation or in explosive environments. In such circumstances optical read-out may be the method of choice. Optical signals can be derived on the basis of tunnelling effects (optical couplers), interference effects (Mach-Zehnder interferometer), (frequency dependent) absorption and polarisation-rotation. When using integrated optics (optical waveguides), a good sensitivity requires the mechanical structures to be within less than a wavelength (0.7-1.5 micrometer) away from the light guides.

As a last sensing principle we mention here the use of tunnelling currents. In this method charges (electrons) do tunnel through a non-conducting gap (e.g. air) from one conductor to another, one of them generally having the shape of a sharp tip. Tunnelling only occurs at small gaps (nanometer sizes) and tunnelling currents are

exponentially dependent on gap distance: $I_t \propto V_b e^{-\alpha_i \sqrt{\phi} x_g}$ with V_b the bias-current, α_i is 1.025, ϕ the effective height of the tunnelling barrier and x_g the gap distance in (Liu et al 1998). To offer a convenient way of detection, tunnelling is often combined with an actuator to form a feedback control keeping the gap distance constant (McCord et al, 1998).

2-2. Variety of micromechanical sensor

Depending on the technologies used and the scale of the mechanical effects one or the other method may be favorable. At here, we mostly introduce the principle of acceleration sensors. There are some types of sensor which classified by their metrical quantity:

- Force sensors
- Pressure sensors
- Load-cells

- Vibration sensors
- Angular rate sensors (gyroscopes)
- Fluid and Flow sensors

2-3. Accelerometers (acceleration sensors)

2-3-1. The definition and applications of accelerometers

An accelerometer is a device that measures acceleration and tilt. Using MEMS technology, accelerometers are widely used in the automotive industry for crash sensing and airbag deployment. The MEMS architectures initially employed in such devices have used a microminiaturized cantilever-type spring, which converts force into a displacement that can be measured. Newer accelerometers use a heated gas bubble with thermal sensors and function much like the air bubble in a construction level. When the accelerometer is tilted or accelerated the sensors pick up the location of the gas bubble. Further information about definition of accelerometers can be obtained from its website (Pcmag-Encyclopedia)

Acceleration sensors come in a variety of sorts both regarding their performance as well as the underlying principles used for sensing. On the rough end of the spectrum one finds the sensors meant to be used e.g. in car as airbag deployment sensors whereas on the other end the very sensitive (micro-g) sensors are found which are intended for use e.g. for seismic applications.

MEMSIC's dual-axis thermal accelerometer works conceptually like the air bubble in a construction level. The square in the middle of the chip is a resistor that heats up a gas bubble. The next larger squares contain thermal couples that sense the location of the heated bubble as the device is tilted or accelerated.

Micromechanical accelerometers are currently produced in such large quantities that

they form the second largest sales volume (following pressure-sensors), a figure mainly due to their large deployment in automotive applications (Yazdi et al, 1998) next to applications in e.g. camera stabilization, active monitoring in biomedical applications, vibration monitoring, three-dimensional mice, headmounted displays for virtual reality, etcetera.

Parameter	Airbag	Vehicle stability	Navigation
Range	50g	2g	1g
Frequency range	0-400 Hz	0-400 Hz	0-100 Hz
Resolution	<100 mg	<10 mg	<4 μ g
Max. shock in 1 ms	>2000 g	>2000 g	>20 g
Off axis sensitivity	<5%	<5%	<0.1%
Temp. Co. of sensitivity	<900 ppm/ $^{\circ}$ C	<900 ppm/ $^{\circ}$ C	<50 ppm/ $^{\circ}$ C

Table (2-1). Specifications of accelerometers for three applications

Basically an accelerometer consists of a mass connected by some kind of suspension to a frame as well as (some degree of) mechanical damping.

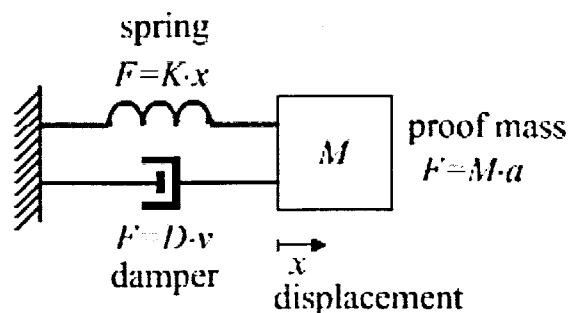


Figure (2-4): Simplified lumped element representation of an accelerometer.

When the frame is accelerated, the mass exerts an inertial force on the suspension leading to a deformation of the suspension and a displacement of the mass relative to the frame of the sensor. Both the deformation of the suspension and the displacement of the proof-mass can be used to obtain a signal, e.g. deformation by strain-gauges and displacement by capacitive effects. The performance of accelerometers is limited by the thermal motion of the proof mass. According to the laws of thermodynamics, the thermal energy of a system in equilibrium is $k_B T/2$ for each energy storage mode, where k_B is the Boltzmann constant and T is the temperature. The small proof mass of micromachined accelerometers results in rather large thermal movements. An equivalent acceleration spectral density, the so-called total noise equivalent acceleration (TNEA) can be calculated and is given by Gabrielson (1993):

$$TNEA = \sqrt{\frac{a_n^2}{\Delta f}} = \frac{\sqrt{4k_B T D}}{M} = \sqrt{\frac{4k_B T \omega_r}{QM}}$$

where Q is the quality-factor and ω_r , the resonance-frequency of the mass-spring-damper system. From this expression it follows that in order to measure low acceleration levels a large proof mass and high quality factor are required.

2-3-2. Some different types of accelerometers

The essential principle of acceleration sensors is similar, but they are classified into many types by the difference of their output value and material:

- Piezoresistive accelerometers
- Capacitive accelerometer
- Pendulous Accelerometer
- Tunnelling accelerometers

- Resonant accelerometers
- Thermal accelerometers

2-3-3. Bandwidth and quality factor, Q , of accelerometers

The bandwidth of an accelerometer refers to its useful range of operating frequencies. This is usually defined by the frequency where the amplitude ratio falls to 0.5, the 3 dB point.

A system's quality factor, Q , describes the sharpness of the system's response. Q is equal to the ratio of the center frequency to the bandwidth. Q is also used to describe the amplitude of the resonant response, which is roughly equal to resonant frequency divided by the driving frequency. Further knowledge about the parameters of accelerometer can be obtained from its website (Capacitive Accelerometers (a))

2-4. Summary

At first, we've done the literature survey about the basic principle of micro-sensor. The elementary principles of most sensors are similar- transform one kind of energy to another in different way, so we can also reference this principle when we design our accelerometer, the key is to find the relationship between input value and output value. And then, we have introduced some typical types of micro-sensor, especially to accelerometer. Some information and characteristics may be used for comparing and referencing in latter work.

Chapter 3

Structure Design and Analysis of Vibration Mode

3-1. Introduction

The main purpose of the structure design is to find a practical and simple structure for this capacitive accelerometer so as to make it convenient for making, and the precondition is working stability. All variable capacitance accelerometers have certain basic design elements in common. They incorporate a seismic mass whose motion in response to shock or vibration lags behind that of the accelerometer housing. The capacitor consists of two plates, one attached to the outer frame and therefore stationary and the other attached to the seismic, or inertial, mass. The value of this capacitor is a function of the distance between the plates, which varies with the motion of the seismic mass.

In this chapter, we will introduce the means of structure design; it includes the element design and the package design. After that, some important typical CA structures will be taken into account for our CA structure design. Some different vibration modes of the structure will be analyzed after the structure is decided. This analysis is mainly for finding the first vibration mode and avoid interfere brought by other vibration modes.

3-2. Design of CA (Connolly, 1995)

3-2-1. CA Element Design

In the silicon differential variable capacitance sensor element, an inertial mass, suspended from either outer layer of the sensor element by a system of multiple flexible beams, undergoes rectilinear movement with applied acceleration.



Figure (3-1): The beams in the suspension system supporting the inertial mass are typically 9 microns wide and 1.5 microns thick.

The mass is electrically connected as part of a variable capacitance half-bridge circuit. Fixed capacitive plates in the lid and base of the sensor element complete the circuit. The capacitance on one side of the circuit increases with acceleration, while the other side proportionally decreases, providing a linearized output.

The sensor element is fabricated by eutectically bonding together three micromachined single-crystal silicon wafers and then dicing the sandwich. Eutectic bonding minimizes the charge migration in the capacitive gaps and the thermal coefficient of expansion mismatch problems that can occur with the more conventional approach of anodic bonding of silicon to Pyrex glass. Both charge migration and relaxation of stress over time due to thermal mismatches can result in zero-bias instability.

The middle layer contains the inertial mass and suspension system. The suspension system (Figure (3-1)) is an array of up to 188 sinuous beams at the levels of the two

principal surfaces of the inertial mass around its rectangular periphery within a supporting frame. Modifications in the shape, cross-sectional area, and number of beams control the suspension stiffness which, in turn, directly affects the device's sensitivity to acceleration. After the beams are laid out on the wafer by high-level boron implantation at particular locations, and with specific geometries, the beams, inertial mass, and ring frame are formed by anisotropic bulk micromachining that etches the wafer from both sides.

3-2-2. CA package design

The package design is optimized for low-cost, high-volume production (see Figure (3-2)). The sensor element is loaded onto a ceramic substrate along with the chip components for its self-contained conditioning circuit. Gold-plated contact pads on the base of the sensor element permit the user to make electrical connections on the circuit board by means of surface-mount technology. The combination of surface-mount technology with chip-and-wire construction facilitates miniaturization of the accelerometer. Long-term stability is ensured by the attachment of a metal lid to the substrate, creating a hermetic environment. The lid is connected to circuit ground for EMI protection.

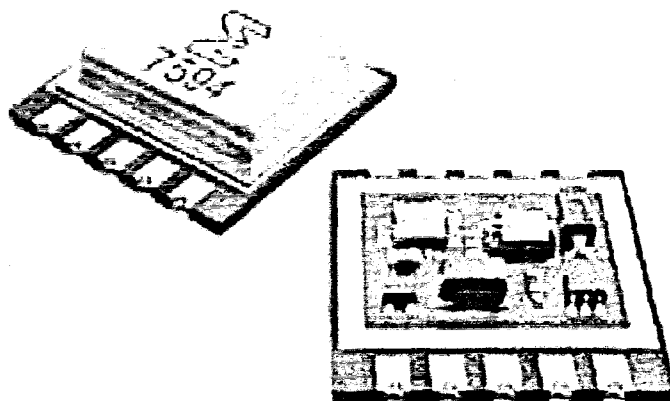


Figure (3-2): The Model 7594 OEM accelerometer is $5/8$ by $5/8$ in. with a height of 0.15 in. The weight is 1.6 g. The cover has been removed to display the sensor element and conditioning circuitry.

Signal conditioning is accomplished by the use of an ultralow-noise CMOS IC with an onchip EEPROM provided to store trim settings. The IC is capable of measurement resolution down to 4.0 aF/Hz. The IC applies a 100 kHz oscillator frequency to the sensor element and detects the change in capacitance between the two capacitive elements within the sensor. This differential signal is then converted to a high-level, low impedance analog voltage output proportional to acceleration.

For unit substitutability, the performance of each device is normalized at the factory by electronically trimming gain and output offset.

The accelerometer in Figure (3-2) operates off 5 VDC excitation with a 5 mA current draw and has a ± 1.75 V differential output swing. An onboard temperature sensor allows users to further improve accuracy by thermal modeling in their system.

3-3. Introduction of some typical structure

3-3-1. Parallel plate CA

Parallel plate CA can be separated into three types according to their different mapping mode of capacitance, and we'll introduce them one by one.

3-3-1-1. Style of distance transformation

For our CA is the CA with style of distance transformation, we just do a simple description on it here.

- **General structure**

The general structure of this type of CA is shown below:

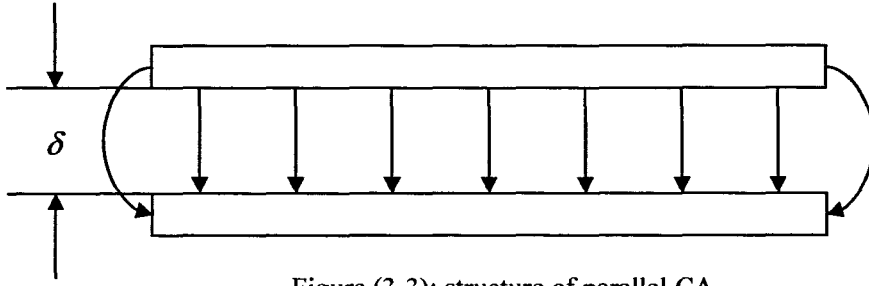


Figure (3-3): structure of parallel CA with style of distance change

● Basic principle

The initial capacitance is

$$C_0 = \frac{\epsilon S}{\delta} \quad (3-1)$$

when the distance (δ) between two poles changes, the capacitance becomes

$$C_1 = \frac{\epsilon S}{\delta - \Delta\delta} \quad (3-2)$$

The relationship between distance (δ) and capacitance (C) is shown in the figure (3-4). It is a linear curve.

and the relative change of capacitance (C) is

$$\Delta C = C_1 - C_0 \quad (3-3)$$

This equation will be expanded in detail within mathematical analysis in chapter 4.

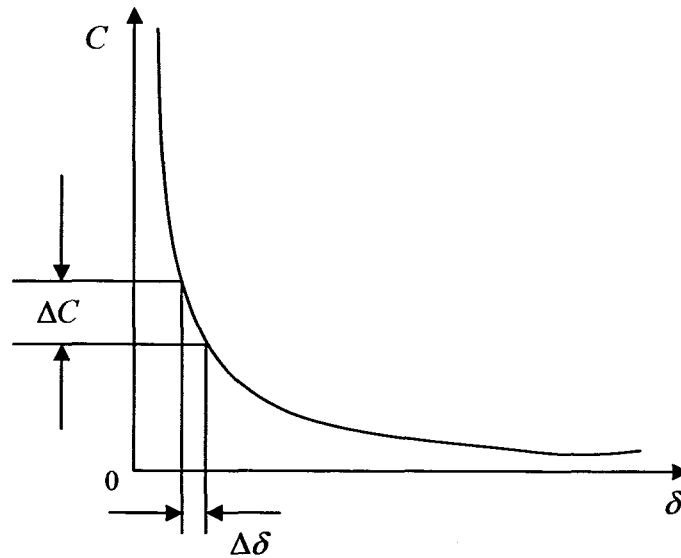


Figure (3-4): the curve of characteristic of $C=f(\delta)$

3-3-1-2. Style of area transformation

The area here is the relative area between two electrode plates. ε and δ both are constants in this CA.

- **Structure**

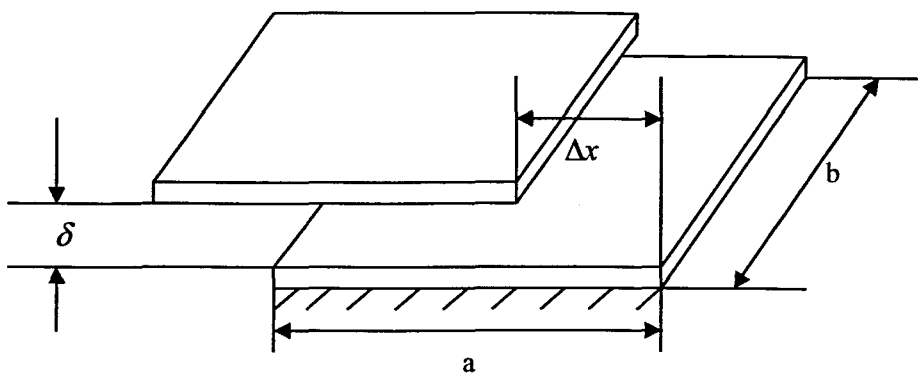


Figure (3-5): structure of parallel CA with style of area change

- **Basic principle**

The initial capacitance is

$$C_0 = \frac{\epsilon s}{\delta} = \frac{\epsilon ab}{\delta} \quad (3-4)$$

when the relative area between two electrodes change, the capacitance becomes

$$\begin{aligned} C_1 &= \frac{\epsilon b(a - \Delta x)}{\delta} \\ &= C_0 - \frac{\epsilon b}{\delta} \Delta x \end{aligned} \quad (3-5)$$

and the relative change of C is

$$\begin{aligned} \Delta C &= C_1 - C_0 \\ &= -C_0 \frac{\Delta x}{a} \end{aligned} \quad (3-6)$$

● Sensitivity

The sensitivity of this kind of CA will be:

$$S = -\frac{\Delta C}{\Delta x} = \frac{\epsilon b}{\delta} = \text{Constant} \quad (3-7)$$

From this equation we know that the sensitivity will go up along with the increase of value of b and decrease of value of δ . On the other hand, the value of another side “ a ” cannot be too small, otherwise the edge effect will augment and the nonlinear error will be amplified sequentially.

Sometimes we like to use teeth-shape for this kind of CA to increase its sensitivity. The figure (3-6) is the transfiguration of figure (3-5). Its purpose is to increase the

covered area.

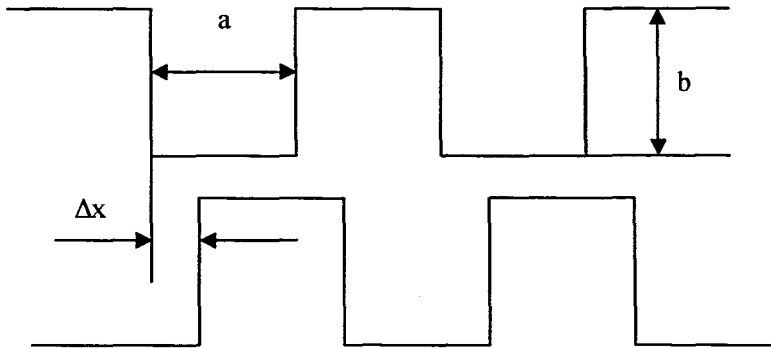


Figure (3-6): structure of teeth-shape

The capacitance of it will be

$$\begin{aligned}
 C_x &= \frac{n\epsilon b(a - \Delta x)}{d} \\
 &= n\left(C_0 - \frac{\epsilon b}{d}\Delta x\right)
 \end{aligned}
 \tag{3-8}$$

The capacitance change is

$$\begin{aligned}
 \Delta C_x &= C_x - nC_0 \\
 &= -\frac{n\epsilon b}{d}\Delta x
 \end{aligned}
 \tag{3-9}$$

So the sensitivity will become

$$\begin{aligned}
 S &= -\frac{\Delta C_x}{\Delta x} \\
 &= n\frac{\epsilon b}{d}
 \end{aligned}
 \tag{3-10}$$

We can see that the sensitivity is n times of original one. But this structure is difficult of making and much more complex.

3-3-1-3. Style of dielectric transformation

For this CA, $\delta = \text{constant}$, $s = \text{constant}$, so $C = f(\epsilon)$,

its structure is shown blow:

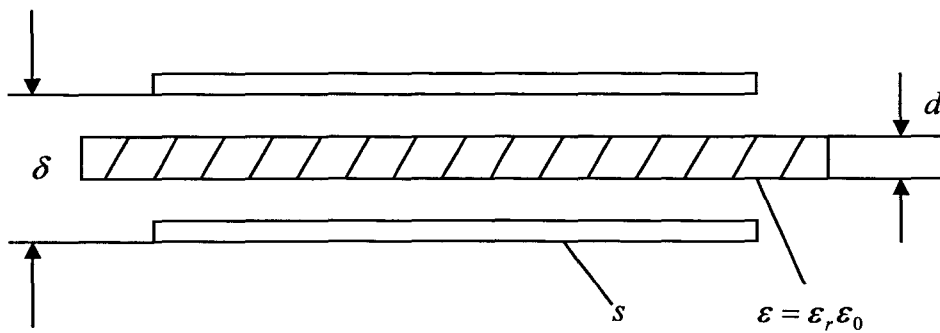


Figure (3-7): structure of parallel CA with style of dielectric change

Obviously, this structure can be considered as two series-wound capacitances, and they are:

$$C_1 = \frac{\epsilon_{r1} \epsilon_0 s}{\delta - d} = \frac{\epsilon s}{\delta - d} \quad (3-11)$$

and

$$C_2 = \frac{\epsilon_0 s}{\frac{d}{\epsilon_{r2}}} \quad (3-12)$$

Total capacitance (C) is

$$C = \frac{C_1 C_2}{C_1 + C_2} = \frac{\epsilon_0 s}{\frac{\delta - d}{\epsilon_{r1}} + \frac{d}{\epsilon_{r2}}} \quad (3-13)$$

Relative dielectric constant of air $\epsilon_{r1} = 1$,

so

$$C = \frac{\epsilon_0 S}{\delta - d + \frac{d}{\epsilon_{r2}}} \quad (3-14)$$

When the thickness of measured solid change, the dielectric constant will become $\Delta\epsilon_{r2}$, and the change of capacitance will be:

$$C + \Delta C = \frac{\epsilon_0 S}{\delta - d + [d/(\epsilon_{r2} + \Delta\epsilon_{r2})]} \quad (3-15)$$

3-3-2. Cylinder CA

- Structure

A and B are two coaxial cylinder conductors. We assume that r is the radius of conductor A; R is radius of B, and $R > r$; L is the length of conductor (Figure (3-8)).

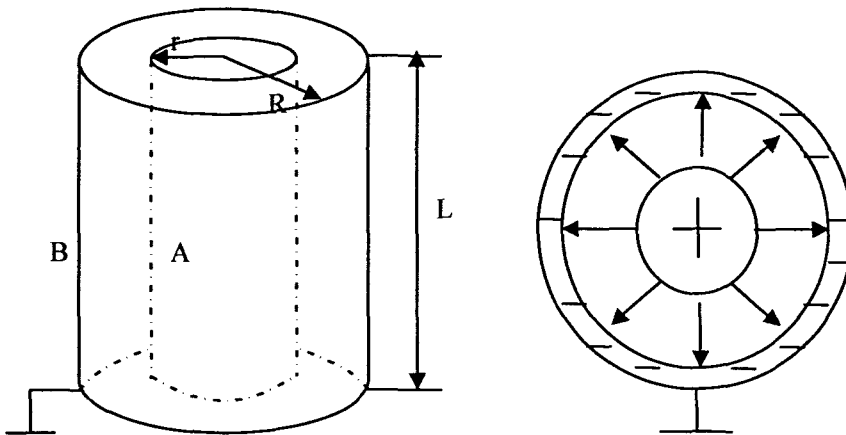


Figure (3-8): coaxial cylinder CA

- **Principle**

When $L \gg R-r$, the edge effect of two sides can be ignored. The intensity of electric field is

$$E = \frac{\lambda}{2\pi\epsilon_0 r} \quad (3-16)$$

The voltage can be calculated as:

$$\begin{aligned} U_{AB} &= \int_A^B E dl \\ &= \int^R \frac{1}{2\pi\epsilon_0} \frac{\lambda}{r} dr \\ &= \frac{\lambda}{2\pi\epsilon_0} \ln \frac{r}{R} \end{aligned} \quad (3-17)$$

λ is the absolute value of charge of every pole at unit length.

The total charge on all poles is $q = \lambda L$

So the capacitance of cylinder CA can be derived from the definition of capacitance:

$$\begin{aligned} C &= \frac{q}{U_{AB}} \\ &= \frac{\lambda L}{\lambda \ln \frac{r}{R} / 2\pi\epsilon_0} \\ &= \frac{2\pi\epsilon_0 L}{\ln \frac{r}{R}} \end{aligned} \quad (3-18)$$

3-4. An example of CA (Garry et al, 2001)

- **Structure**

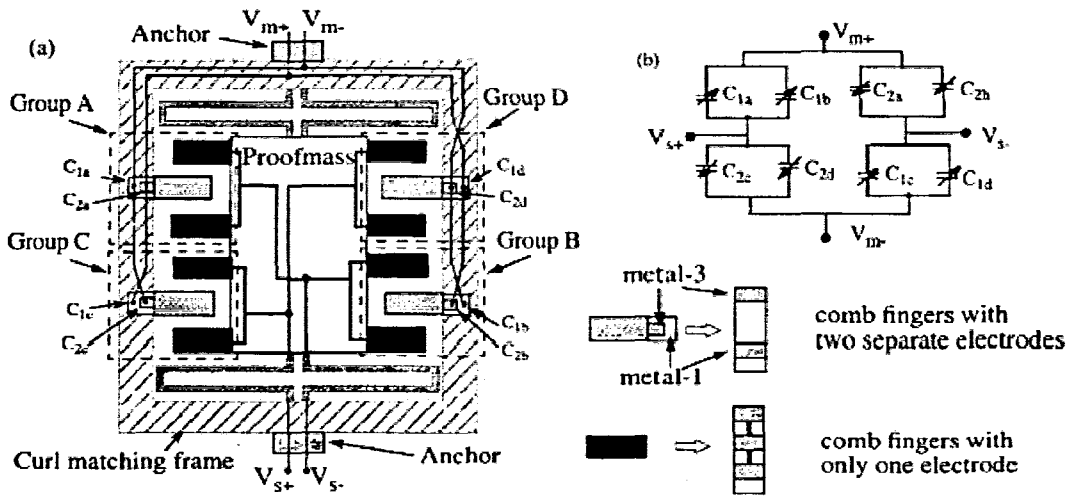


Figure (3-9): Topology design and wiring configuration of the z-axis accelerometer.

In Figure (3-9), (a) is Schematic of the top view of the layout with a common-centroid configuration. (b) is Equivalent full-bridge differential capacitive interface.

● Operational principle

Let's see a picture of principle first:

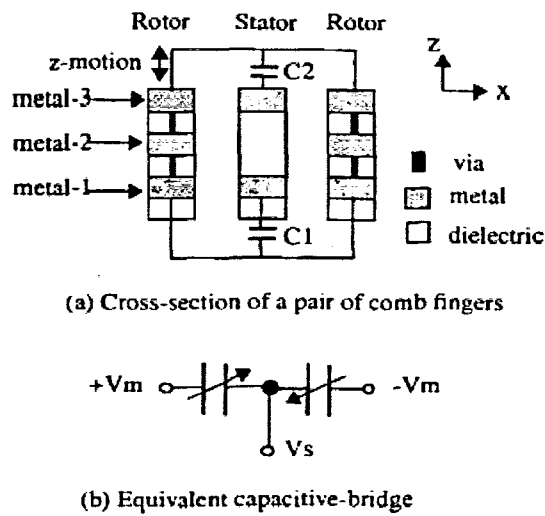


Figure (3-10): principle of z-displacement capacitive-sensing through comb-finger

The cross-section of pair of multi-conductor comb-finger is shown in the figure above; the stator finger is constructed of metal-1 and metal-3 layers which are insulated by oxide, while the rotor finger includes three metal layers which are electrically connected together. Two sidewall capacitors C1 and C2 are formed. When the rotor finger moves up or down, C1 and C2 will change value in opposite direction.

If balanced modulation voltages $\pm V_m$ are applied, the output signal V_s is expressed as:

$$V_s = \frac{C_1 - C_2}{C_1 + C_2} V_m \quad (3-19)$$

- **The parameters of this CA**

	Designed	Measured
Dimension	500x500 mm ²	-
Resonant frequency	10.1kHz	9.4kHz
Quality factor in air	-	3
Sensor sensitivity	0.75mV/g/V	0.5mV/g/V
Cross-sensitivity	-55dB	<-40 dB
Linear range	+/-600g	+/-27g
Noise floor	0.6 mg/rtHz (Brownian; Q=3)	6 mg/rtHz

Table (3-1): The characteristics of Differential CA with comb-fingers

3-5. The analysis of these types of CA

First of all, our purpose and idea of our work is to design a capacitive accelerometer

which can work stably. On the other hand, the factor of economy and fabrication can not be ignored too.

From the contrast of those types of CAs, we can easily see that the working principle and structure are approximately same, and the sensitivities of them are similar too. The most obvious difference between them is working manner. Out of consideration for cost and the manufacturing of our CA, the parallel plate CA with the style of distance transformation is the best choice for us. Next we'll introduce the structure of our CA.

3-6. Introduction of the structure of our CA

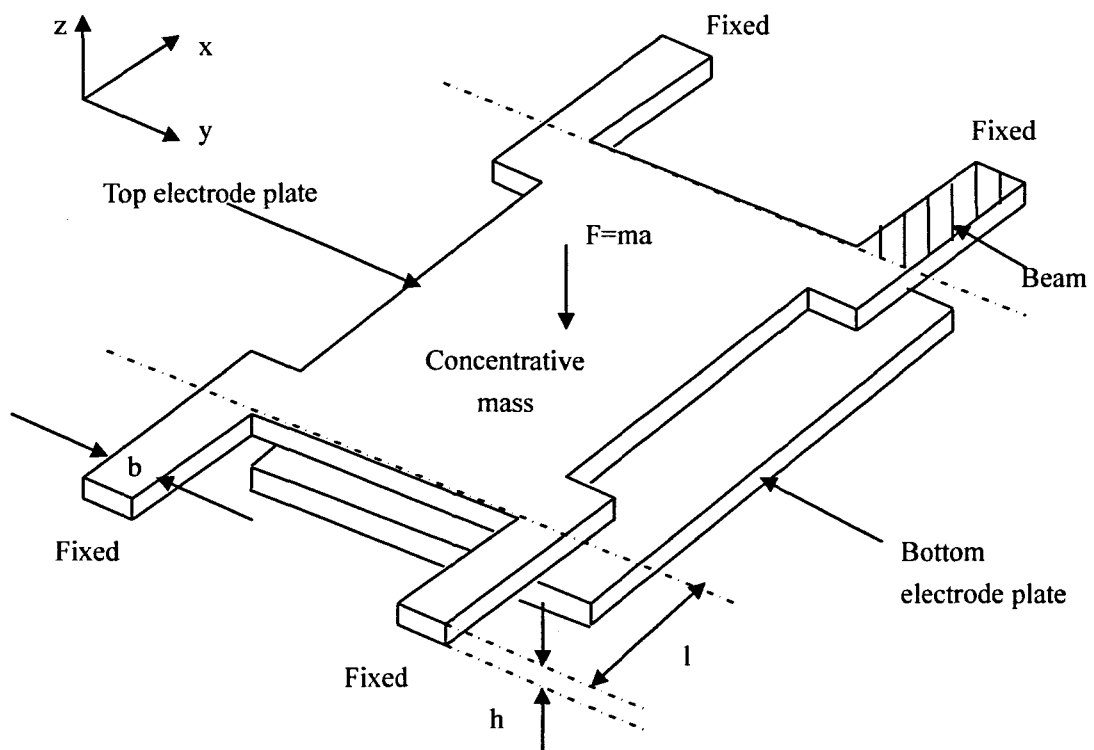


Figure (3-11): capacitive accelerometer with crab-shape structure

First of all, I use a picture above to show the structure of my capacitive accelerometer and some important features of it. Out of consideration for the stability of this

structure we design its configuration as four fixed symmetric beams and a central proof mass.

The medium part between the two pieces of long broken line is a concentrative mass. The purpose of design of the mass shape is to reduce edge effect of this structure, and the part with shade is beam which is fixed at the end of it. The rest of three beams are same. The measurement of beams has been shown as b , h , and l in the figure above (b --width of beam, h --thickness of beam, l --length of beam). We can also see that the concentrative mass is receiving a force which magnitude should be the product of m (mass) and a (acceleration).

where $m = \rho v$ (ρ (density), v (volume)). On the other hand, there is C (capacitance) between the two electrode plates, and $C = \frac{\epsilon s}{\delta}$, where ϵ (constant of medium), s (relative area of two plates), δ (distance between two plates)

3-7. Analysis of vibration mode (simulated by CoventorWare)

The measurement and some important parameters must be calculated through the mathematical analysis of the structure. But we can not analyze all vibration modes of this structure; we only study the first or main vibration mode of it. So next we will do simulation by using CoventorWare and confirm which mode is the mode we need to analyze.

3-7-1. Process setting:

CoventorWare provides a database for storing all material properties likely to be used in a solver calculation. This data is stored in the *.mpd* file, which is placed in a folder named *MPD* in the user's shared directory when any material is selected; its physical properties are automatically displayed. The layers identified in the layer browser are

referred to as *Masks* in the *Process Editor*. The process is chronological from the top down (Figure(3-12)).

Step	Action	Type	Layer Name	Material	Thickness	Color	Polarit y	Depth	Offset	Sidewall Angle	Cor
0	Base		Substrate	SILICON	10.0	blue	GND				
1	Deposit	Stacked	Nitride	SIN	0.2	gold					
2	Deposit	Stacked	Sacrifice	BPSG	2.0	green					
3	Etch	Front, Last L...				blue	anchor -	2.0	0.0	0.0	
4	Deposit	Conformal	beam	ALUMINUM(FILM)	0.5	red	(SCF)				
5	Etch	Front, Last L...				red	beam +	0.5	0.0	0.0	
6	Sacrif...			BPSG							

Figure (3-12): the design of process of MEMS

We can see that the whole MEMS course is shown in the figure above; they include deposit, etch and sacrifice etc. After this process, we draw a 2D layout for each layer and then the CoventorWare can create a 3D graph automatically from the 2D layout that we draw in front.

3-7-2. 2-D layout

After we finish the input of parameters in each process, the work should be done next is to draw a 2-D layout for each layer. (Base, Nitride, bottom electrode plate, Sacrifice, top electrode plate)

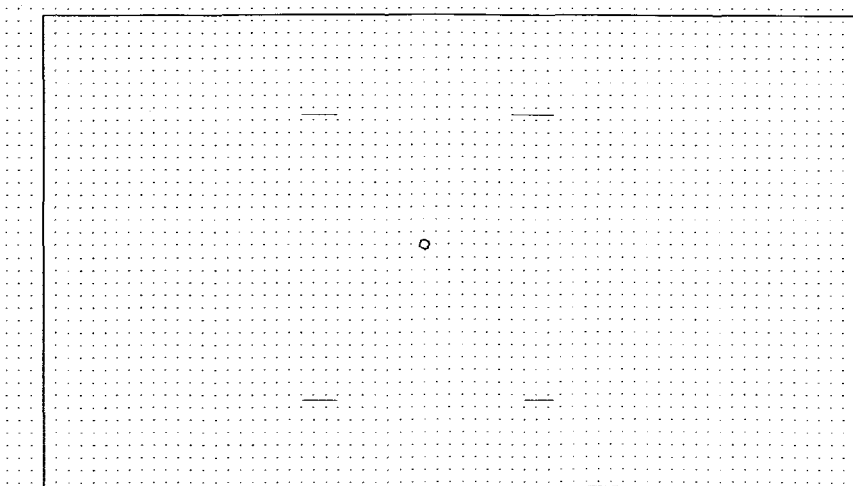


Figure (3-13): the 2-D layout of the structure

3-7-3. Creation of mesh

For doing latter analysis, such as the analysis of finite element and resonant frequency, we need to create a mesh mode for the 3D model.

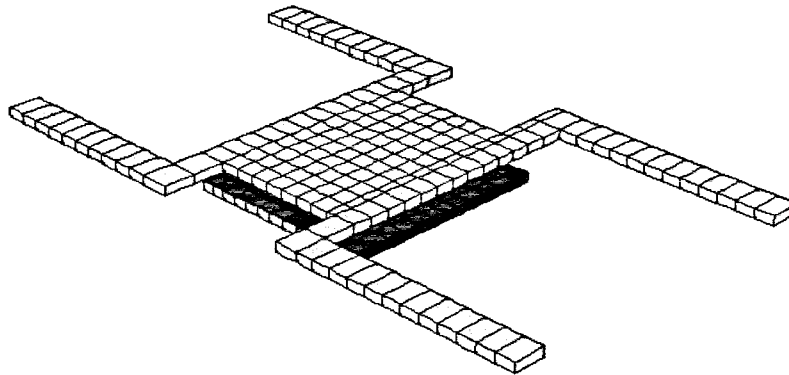


Figure (3-14): the mesh mode of the structure

3-7-4. Simulation of vibration modes

We can simulate numberless mode of the structure through the function of simulation. But few simulations are enough. We only simulate 6 modes here.

3-7-4-1. The 1st vibration mode:

By using CoventorWare's function of analysis, we can simulate the movement of this 3-D structure, and attain the table of some important parameters to define the first or main movement. This picture can show us the situation of whole structure when it vibrates up to ultimate position.

This vibration mode is vibrating up and down; it exactly is what we need for defining the change of capacitance. So we can find the acceleration through the math mode we create in next chapter.

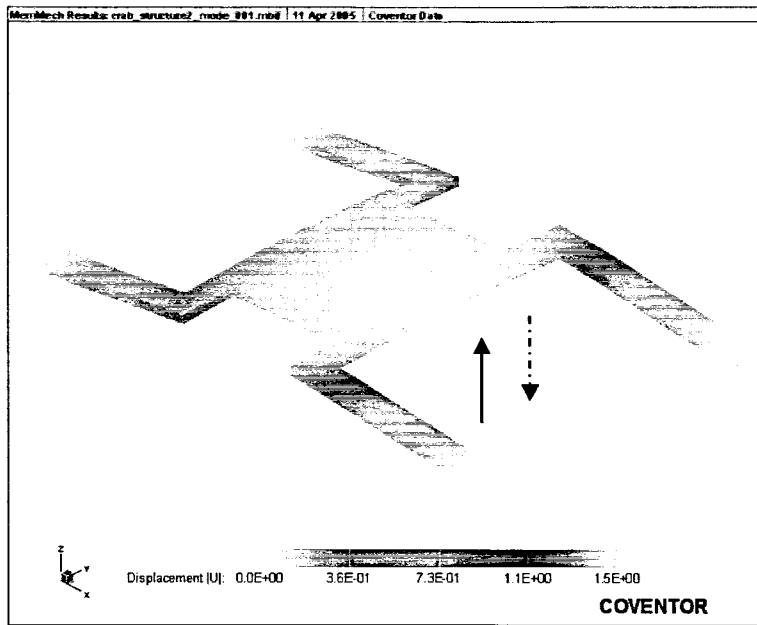


Figure (3-15): The 1st vibration mode of the structure

We can see that the vibration mode in this figure is most familiar and can occur most possibly. We will do the analysis of resonant frequency for it to confirming that this vibration mode is the first (main) mode.

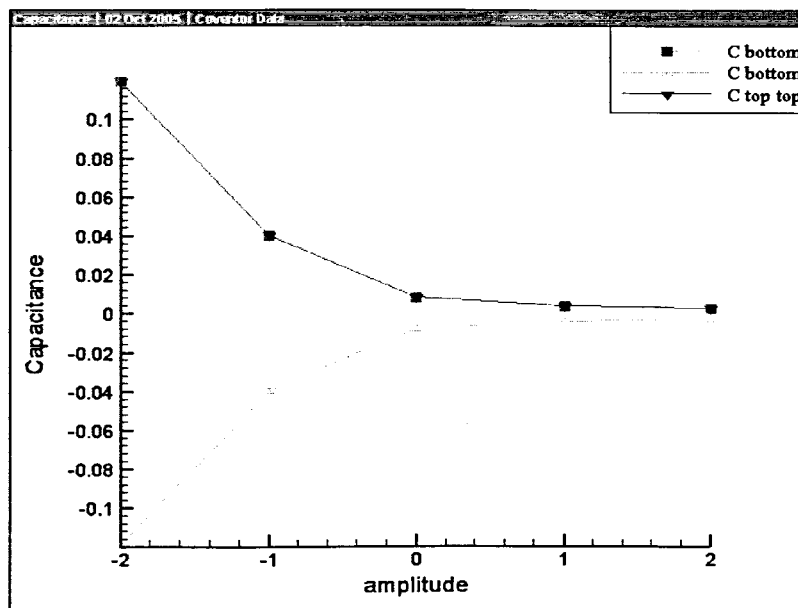


Figure (3-16): the graph of capacitive change of first mode

At the same time, CoventorWare can output the picture above; we can see that the change of capacitance of first mode is linear. That is also the symbol of first or main

vibration mode.

3-7-4-2. The rest of vibration modes:

The arrows shown in those pictures denote the direction of motion.

- **The 2nd vibration mode:**

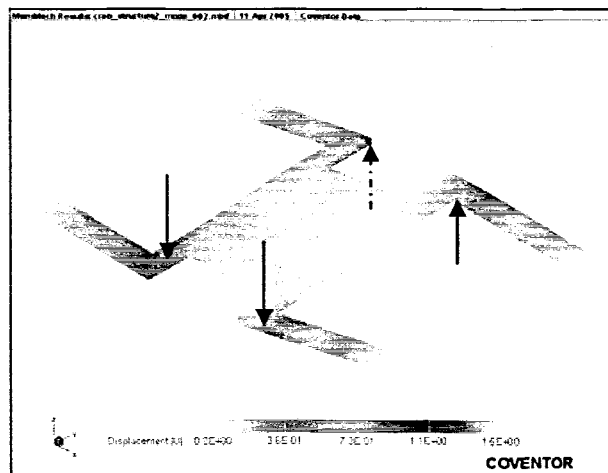


Figure (3-17): The 2nd vibration mode

- **The 3rd vibration mode:**

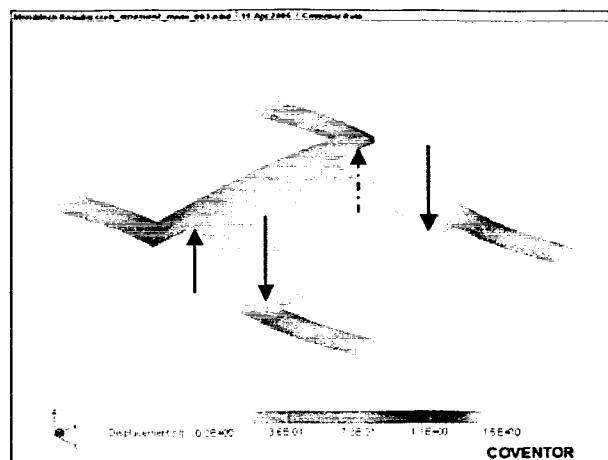


Figure (3-18): The 3rd vibration mode

- The 4th vibration mode:

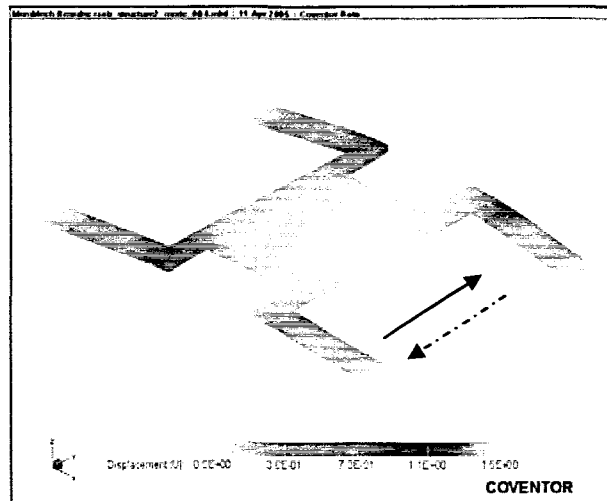


Figure (3-19): The 4th vibration mode

Note: the structure in this mode is vibrating from left to right horizontally. For the area of bottom plate is bigger than top one, the relative area between two plates will be invariable.

- The 5th vibration mode:

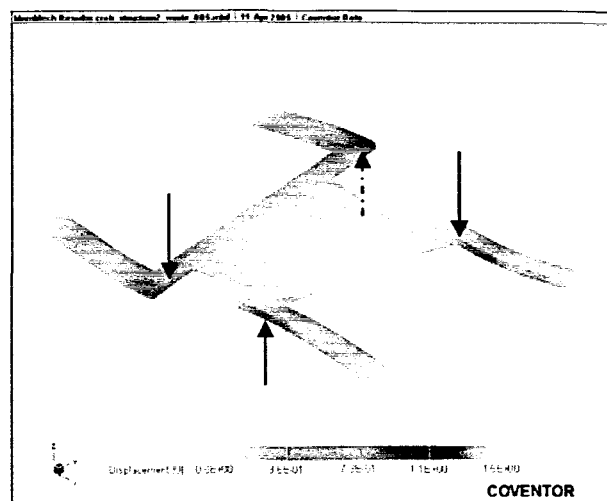


Figure (3-20): The 5th vibration mode

● The 6th vibration mode:

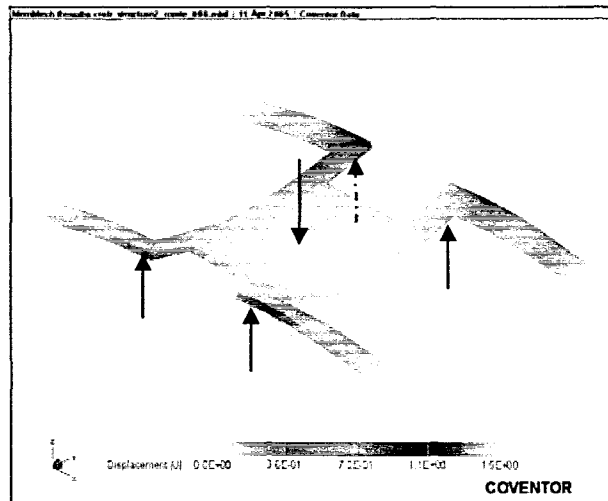


Figure (3-21): The 6th vibration mode

3-7-5. Analysis of six modes

Through the modal analysis of CoventorWare, we can attain a table of six frequencies of all modes that we have described above. In fact, there are many kinds of analysis that we can do to these six modes, but now we only need to distinguish which mode is the first or main mode that we need to do more particular analysis, so the table below which is showing the frequencies of six modes is enough for us.

modeDomain	Frequency	Generalized Mass	Damping
1	1.044086E05	6.919874E-09	0.0
2	1.865338E05	7.508392E-09	0.0
3	2.676600E05	3.705959E-09	0.0
4	3.335556E05	4.657062E-09	0.0
5	5.670923E05	3.572520E-09	0.0
6	6.711327E05	3.911652E-09	0.0

Close

Table (3-2): frequencies in six modeDomains

We can see from the table above that the first mode's natural frequency is smallest among six modes. As we know the vibration mode with lower frequency will occur easier than others, so it is easy to say that the first vibration form with lowest natural frequency is the main mode that we need to analyze.

After we find the first vibration mode, we need to think how to eliminate the other mode's disturbance of change of capacitance.

In addition to the first mode, other vibration modes don't have absolute but relative change of distance between two electrodes. For example, see Figure (3-22).

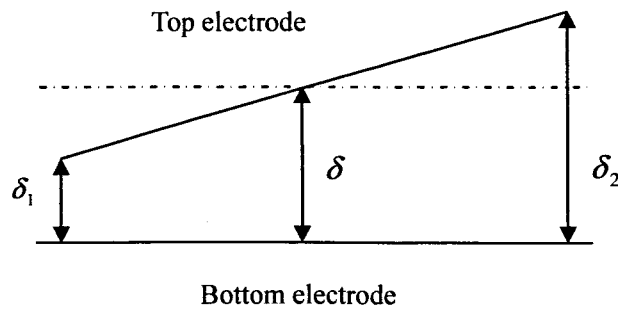


Figure (3-22): the relative change of distance

We can see from this figure that the capacitance will keep same when we calculate capacitance by distance integral. The situations of other vibration modes are mainly same. So the disturbance of other five modes can be ignored automatically. That also means that the other modes can not effect on the change of capacitance.

3-8. Summary

From many familiar structures of CA, we choose the parallel one as our CA's structure because of its practicability and simplicity. Furthermore this structure has already been developed for increasing its working efficiency and accuracy. By the

design of crab-shape, the edge effect has been reduced. The stability of this structure is also high for the design of four symmetrical beams with fixed ends. Through the analysis of vibration modes we can define a first vibration mode to analyze in following chapter. This also means that this structure is easily to analyzing and making because of its simplicity of motion.

Although the complex structure can increase the capability of accelerometer generally, it will bring complex or synthetical motion too. And thereby the structure will be very difficult of analysis and making.

Chapter 4

Establishment of Math Model and Mathematical Analysis

4-1. Introduction

Generally, the two important parameters in evaluating accelerometer sensors are sensitivity and operating frequency range. Sensitivity can be defined as the capacitance per unit acceleration ($S = \frac{\Delta C}{a}$). Operating frequency range is the flat frequency response region below the fundamental resonance frequency of the sensor.

There're still many other parameters which will be considered by users and customers when they try to choose an appropriate sensor for themselves, whereas the type of contemporaneity sensor differs in thousands ways. And it is impossible that all targets accord with the requirement of users' only by choosing one type of sensor. So which kind of sensor they will buy must depend upon the purpose, object and condition of measurement.

The central task of this chapter is to define the measurement of this crab-shape structure to improve the performance of it. Some useful mathematical analysis, static and dynamic analysis will be used for confirming some important parameters after the math model is created. And then we will compare these parameters with existing products to verifying its working capabilities.

4-2. Mechanics analysis of static model

4-2-1. Purpose of analysis

To all capacitive accelerometers, the input value is acceleration and the output value is capacitance. So our purpose of doing this analysis of static model is to find the relationship between ΔC (the change of capacitance) and a (acceleration). At last, we try to find a way in which the acceleration is denoted by the change of capacitance. For instance, $a = (\dots) \Delta C$.

During the whole course of research, the capacitance is a known quantity and the acceleration is an unknown quantity. So our primary aim of following analysis is to find the relation between a (acceleration) and ΔC (change of capacitance).

4-2-2. Analysis

4-2-2-1. The analysis of structure

Note: Before we do this analysis, there is a necessary step we must do first. That should be the analysis of vibrational mode—to decide which form is the first vibration form and why we use it for analysis. And this analysis has already been done by using the CoventerWare (one kind of simulative and analytical software which is especially for MEMS production design) at the fore. So the posterior analysis and calculation will be all fixed attention on the first vibration mode.

First of all, we must simplify this structure. For several conditions are satisfied, we can divide the whole structure into two symmetrical parts. (Conditions: 1. the medium is regarded as vacuum, 2. the material is well-proportioned, 3. the boundary condition of two sides are same, 4. the whole structure is symmetrical)

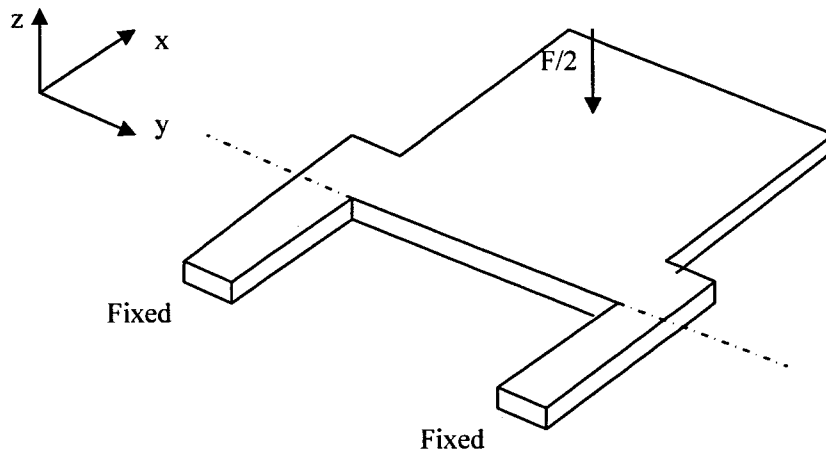


Figure (4-1): Separate it into two parts

For each part, it receives $F/2$ force, viz. $ma/2$.

4-2-2-2. The analysis of force

Next, we will concentrate upon one beam because key quantity that affects the change of capacitance is displacement of top plate. And the displacement of top plate is namely the displacement of the free end of beams for the concentrative mass will not bend. Now we just see one beam and analyze it.

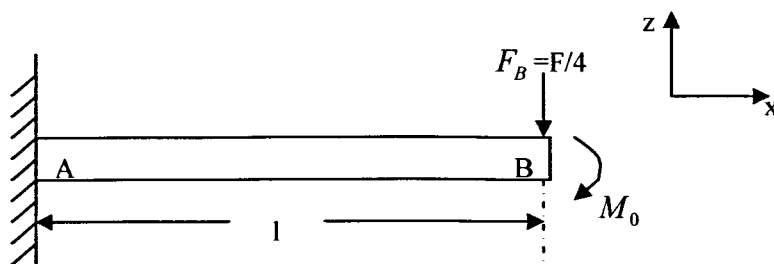


Figure (4-2): Status of force and bending moment act on the beam

M_0 is an assumptive bending moment. The real bending moment is M .

$$M = M_0 - \frac{1}{4}Fx \quad (4-1)$$

Under the action on the beam, finally the beam's deformation is shown below

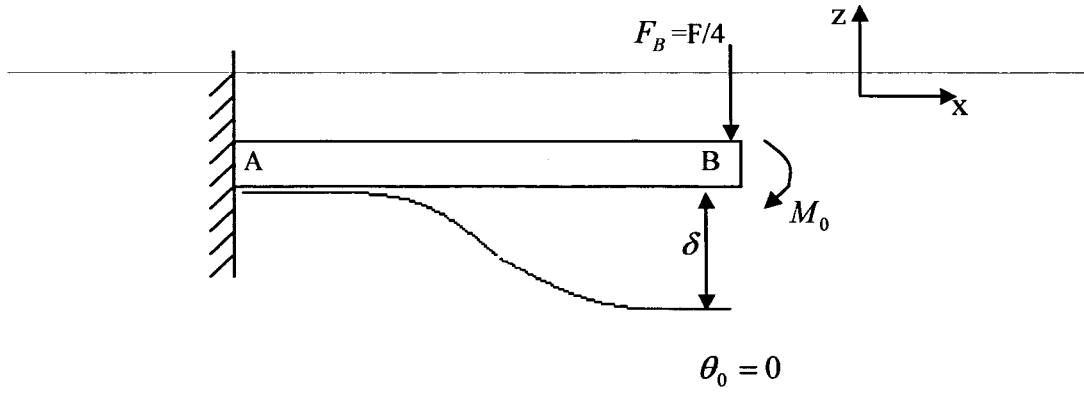


Figure (4-3): The deformation of the beam

We can see that the rotation angle of the end which connects with concentrative mass is still zero when the displacement goes up to max. (δ is the max displacement)

In terms of the particularity of this structure (two sides fixed), we use the theorem of energy--*Castigliano's Theorem* to require the max displacement of the beam in succession.

● Strain energy

The denotation of strain energy is U.

$$U = \int_0^l \frac{M^2}{2EI_z} dx \quad (4-2)$$

I_z is the moment of inertia to the axis Z.

$$I_z = \frac{bh^3}{12} \quad (4-3)$$

- Apply $\theta_0 = 0$ to require bending moment

$$\begin{aligned} \theta_0 &= \frac{\partial U}{\partial M_0} \\ &= \int_0^l \frac{M}{EI_z} \frac{\partial M}{\partial M_0} dx \\ &= \frac{1}{EI_z} \int_0^l \left(M_0 - \frac{1}{4}Fx \right) dx = 0 \end{aligned} \quad (4-4)$$

By solving this equation, we have:

$$\begin{aligned} M_0 &= \frac{1}{8}Fl \\ M &= \frac{1}{8}Fl - \frac{1}{4}Fx = \frac{1}{4}F\left(\frac{l}{2} - x\right) \end{aligned} \quad (4-5)$$

- Max displacement

$$\begin{aligned} \delta &= \frac{\partial U}{\partial F_B} \int_0^l \frac{M}{EI_z} \frac{\partial M}{\partial F_B} dx \\ &= \frac{F}{4EI_z} \int_0^l \left(\frac{l}{2} - x\right)^2 dx \\ &= \frac{Fl^3}{48EI_z} \end{aligned} \quad (4-6)$$

And then substitute (1-3) into this equation, we finally have:

$$\delta = \frac{Fl^3}{4Ebh^3} = \Delta\delta \quad (4-7)$$

Substitute $F = ma$ into this formula:

$$\Delta\delta = \frac{mal^3}{4Ebh^3} \quad (4-8)$$

4-2-2-3. Find the relationship between acceleration and capacitance

- Initial capacitance is C_0

$$C_0 = \frac{\varepsilon_0 s}{\delta_0} \quad (4-9)$$

ε_0 is dielectric constant; s is relative area between two plates; δ_0 is initial distance between two plates.

Note: During the course of design, we can keep the relative area between two plates' unchangeable, if only the area of bottom plate (s_b) is bigger enough than the area of top plate (s_t). So we only pay attention to the change of distance between two plates.

- The capacitance after δ_0 has changed (C_1)

$$C_1 = \frac{\varepsilon_0 s}{\delta_0 - \Delta\delta} \quad (4-10)$$

Substitute $\Delta\delta$ into this formula, we have:

$$C_1 = \frac{4\varepsilon_0 s E b^3 h}{4Ebh^3 \delta_0 - mal^3} \quad (4-11)$$

So we can require the change of capacitance:

$$\begin{aligned}\Delta C &= C_1 - C_0 \\ &= \frac{4\varepsilon_0 s E b^3 h}{4Ebh^3\delta_0 - ma^3} - \frac{\varepsilon_0 s}{\delta_0} \\ &= \frac{ma^3 \varepsilon_0 s}{4Ebh^3\delta_0^2 - ma^3\delta_0}\end{aligned}\quad (4-12)$$

And then we hope that the result is a linear expression, so we do the next work to simplify this complex result to attain a linear expression.

The relative change of capacitance is $\frac{\Delta C}{C_0}$:

$$\begin{aligned}\frac{\Delta C}{C_0} &= \frac{C_1 - C_0}{C_0} \\ &= \frac{\Delta\delta}{\delta_0} \left(1 - \frac{\Delta\delta}{\delta_0}\right)^{-1}\end{aligned}\quad (4-13)$$

When the expression $\frac{\Delta\delta}{\delta_0} \ll 1$ comes into existence, we can do a transform through

Fourier series to simplify it.

At first, we spread $\left(1 - \frac{\Delta\delta}{\delta_0}\right)^{-1}$ into a Fourier series:

$$\left(1 - \frac{\Delta\delta}{\delta_0}\right)^{-1} = 1 + \frac{\Delta\delta}{\delta_0} + \left(\frac{\Delta\delta}{\delta_0}\right)^2 + \left(\frac{\Delta\delta}{\delta_0}\right)^3 + \dots + \left(\frac{\Delta\delta}{\delta_0}\right)^n \quad (4-14)$$

This formula is nonlinear, so we just omit nonlinear terms and then we have an

approximate formula:

$$\frac{\Delta C}{C_0} \approx \frac{\Delta \delta}{\delta_0} \quad (4-15)$$

So finally we obtain the linear relationship between acceleration (a) and change of capacitance (ΔC):

$$a = \frac{4Ebh^3 \delta_0^2}{ml^3 \epsilon_0 s} \Delta C \quad (4-16)$$

$$\Delta C = \frac{ml^3 \epsilon_0 s}{4Ebh^3 \delta_0^2} a \quad (4-17)$$

4-2-3. Sensitivity

4-2-3-1. The definition of sensitivity (Madou, 2005)

A sensor detects information input I_{in} , and then transduces or converts it to a more convenient form I_{out} . (i.e. $I_{out} = f(I_{in})$). So sensitivity is the amount of change in a sensor's output in response to a change at a sensor's input over the sensor's entire range.

Very often sensitivity approximates a constant; that is, the output is a linear function of the input

Sensitivity may mathematically be expressed as:

$$\eta = \frac{dI_{out}}{dI_{in}} \quad (4-18)$$

There is an example of temp sensor's sensitivity (Figure (4-4)).

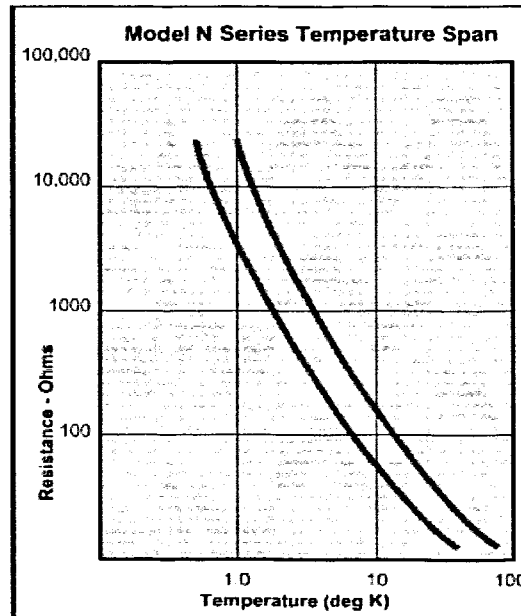


Figure (4-4): Sensitivity 35,000 Ohms/K @ 4.2 K

4-2-3-2. The sensitivity's calculation

Sensitivity is a very important and practical parameter of sensors. It will be the most first feature that customers and users care when they choose one type of sensor. So we must find and confirm the accurate range of sensitivity of our accelerometer.

Generally, at the linear range of sensors, we hope that the sensitivity of sensor can be as high as possible. None but the value range of output signal is large; the signal can be dealt with easily. But on the other hand, disturbance of noise will be more when sensitivity is high, sequentially effect precision of sensor. Thus we must pay attention to the precision of sensor when we try to improve the sensitivity.

The sensitivity is defined for our accelerometer as:

$$S = \frac{\Delta C}{a} \quad (4-19)$$

And then we substitute ΔC and $\Delta \delta$ into this equation, we have:

$$S = \frac{\frac{ml^3 \varepsilon_0 s}{4Eb^3 \delta_0^2} a}{a} \quad (4-20)$$

$$= \frac{ml^3 \varepsilon_0 s}{4Eb^3 \delta_0^2}$$

Sometimes to improve the sensitivity of sensors, we can adopt difference configuration. That is a more complicated structure than that we are using now.

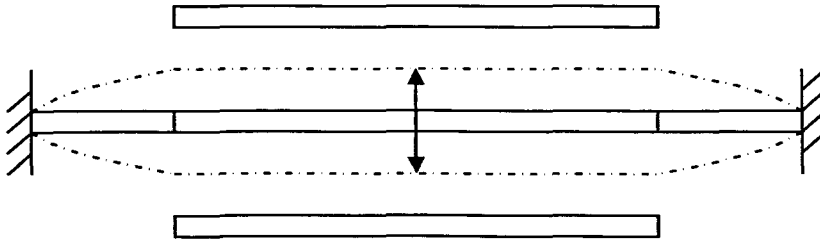


Figure (4-5): the sketch map of difference configuration

When the central plates moves up and down, the capacitance between upper and lower plate will change at same time. At this time, the sensitivity will equal to two times of S which we have acquired already.

$$S' = 2S = 2 \frac{\Delta C}{a} \quad (4-21)$$

This structure can improve the sensitivity, but for the precision of our sensor, we only use the first structure that we have introduced above

4-2-4. Resonant frequency

In sound applications, a resonant frequency is a natural frequency of vibration determined by the physical parameters of the vibrating object. This same basic idea of physically determined natural frequencies applies throughout physics in mechanics, electricity and magnetism, and even throughout the realm of modern physics.

It is also an important measurement which is using for measuring stand or fall of an accelerometer. Under the most general standard, an accelerometer will be considered as better as its resonant frequency is lower. So it becomes very pivotal that how to reduce the natural frequency of accelerometer furthest.

As we know the natural frequency (resonant frequency) of a vibration system is:

$$\omega_n = \sqrt{\frac{k}{m}} \quad (4-22)$$

where k is elastic coefficient, and m is the mass of vibration plate.

And we know that the elastic coefficient k can be calculated by the equation below:

$$k = \frac{f}{x} \quad (4-23)$$

where f is the force which acts on plate, x is the displacement of plate.

4-3. Dynamic analysis

4-3-1. dynamic mathematical model (Qing-Ming Wang, 2004)

First of all, we simplify the whole model to do the dynamic analysis

The dynamic model can be simplified as a beam with a large mass (half of the

concentrative mass m) in the center, and subjected to a periodic force $f(t)$, as shown schematically by Fig (4-6). The sinusoidal force can be written as:

$$f(t) = \frac{1}{2} mg \sin 2\pi ft \quad (4-24)$$

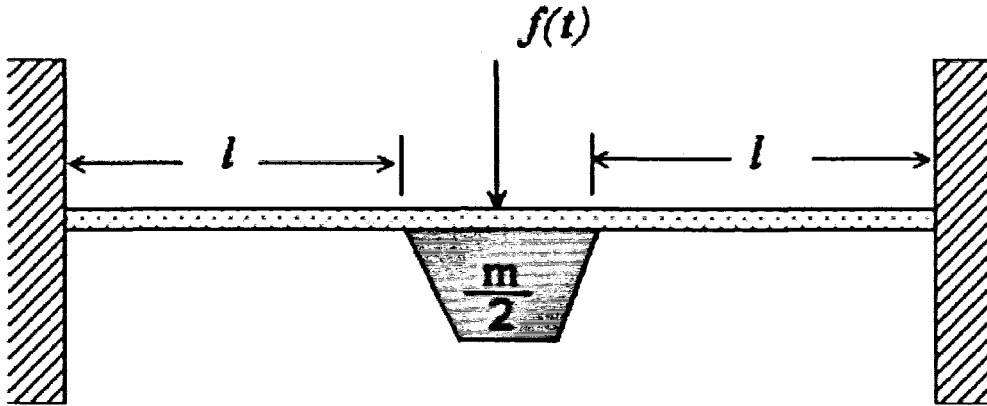


Figure (4-6): Dynamic model of accelerometer

Where $g = 9.8 \text{ m/s}$ and f is the driving frequency.

Assuming that the accelerometer is at rest initially, if only the first vibration mode is considered here, the general solution of the beam is given by McCallion (1973):

$$z(x) = a_1 \cos(\beta x) + a_2 \sin(\beta x) + a_3 \cosh(\beta x) + a_4 \sinh(\beta x) \quad (4-25)$$

Where a_1 , a_2 , a_3 , a_4 and β are the constants.

From the boundary conditions

$$\begin{aligned} x=0 & & x=0 \\ y(0) = y'(0) = 0 & & y(l) = y'(l) = 0 \end{aligned}$$

The first normal mode of the accelerometer can be obtained as:

$$z_1(x) = V_a [\sin kx - \sinh kx + S(\cos kx - \cosh kx)] = V_a g(x) \quad (4-26)$$

Where

$$k = 4.73 / 2l \quad (4-27)$$

$$S = \frac{\sinh kl - \sin kl}{\cos kl - \cosh kl} \quad (4-28)$$

And V_a is the constant.

Since the first normal is orthogonal, V_a can be obtained by:

$$\int_0^{2l} \gamma(x) A(x) z_1^2(x) dx = 1 \quad (4-29)$$

where $\gamma(x)$ is the density and A is the cross-sectional area.

Considering that the concentrative mass m is much larger than the mass of the beams, the above equation can then be simplified to give:

$$V_a = \sqrt{\frac{1}{m/2g^2(l)}} \quad (4-30)$$

From Rayleigh method (A method used for calculating approximate natural frequencies for a vibrating system assuming a deflected shape and balancing kinetic and strain energies.), the fundamental natural frequency f_n is given by:

$$f_n^2 = \frac{2}{4} \int_0^l \frac{dU_{\max}}{\pi^2 K_{e\max}} \quad (4-31)$$

Where

$$K_{e\max} = \frac{1}{2} m z_1^2(l) \quad (4-32)$$

And dU_{\max} will change along with the change of material and structure of model.

Using the expansion theorem, the displacement of the capacitive accelerometer can be written as:

$$z(x, t) = z_1(x)\eta(t) \quad (4-33)$$

where $\eta(t)$ is the modal coordinate which is expressed by the form of convolution.

$$\eta(t) = \frac{1}{2\pi f_n} \int_0^t N(\tau) \sin(2\pi f_n)(t - \tau) d\tau \quad (4-34)$$

where N is the modal force given by

$$N(t) = \int_0^l z_1(x) f(x, t) dx \quad (4-35)$$

At last, substituting (4-26), (4-34), (4-35) into (4-33) we finally have:

$$z(x, t) = \frac{V_a^2}{2} mgz(l) \frac{\sin 2\pi ft - (f / f_n) \sin 2\pi f_n t}{(2\pi f_n)^2 - (2\pi f)^2} \times [\sin kx - \sinh kx + S(\cos kx - \cosh kx)] \quad (4-36)$$

Substituting the equation (4-36) into (4-9), we can acquire the dynamic equation of capacitive

$$C = \frac{2\epsilon S [(2\pi f_n)^2 - (2\pi f)^2]}{V_a^2 mgz(l) [\sin 2\pi ft - (f / f_n)] \times [\sin kx - \sinh kx + S(\cos kx - \cosh kx)]} \quad (4-37)$$

Using this equation, the capacitive change (ΔC) and acceleration (a) of the device

under dynamic excitation can be predicted.

Substituting (4-36) into (4-17), then we have the instantaneous expression of acceleration and change of capacitance:

$$\Delta C = \frac{2[(2\pi f_n)^2 - (2\pi f)^2] \gamma l^3 \varepsilon_0 s}{4Ebh^3 \delta_0^2 V_a^2 mgz(l) [\sin 2\pi ft - (f/f_n)] \times [\sin kx - \sinh kx + S(\cos kx - \cosh kx)]} a \quad (4-38)$$

4-3-2. Stress analysis

From equation $M = M_0 - \frac{1}{2}Fx$, we can see that the maximum of moment is at $x = 0$.

Assuming that there is only vertical acceleration applied to the central proof mass, the beams are primarily subjected to stresses in one direction, and other stresses can be ignored because they are too small. Therefore, the maximum stress can be obtained by using the equation below:

$$\sigma_{\max} = \frac{M_{\max}}{W} \leq [\sigma] \quad (4-39)$$

where M_{\max} is the maximum bending moment and W is the coefficient of resistance of bending in cross section.

The value of $[\sigma]$ can be obtained from the table below.

Parameters	Silicon
Young's modulus (N/m^2)	1.9×10^{11}
Poisson's ratio	0.18
Density (kg/m^3)	2330
Fracture strength (N/m^2)	7×10^9
($\epsilon_0 = 8.85 \times 10^{-12}$ in vacuum)	730

Table (4-1): Part of characters of silicon

The fracture strength which is shown in the table is $[\sigma]$.

And then the max acceleration could be derived from the steps which are shown below:

$$M = \frac{1}{4} F \left(\frac{l}{2} - x \right) \quad (4-40)$$

For σ_{\max} is at where $x = 0$,

$$\begin{aligned} M_{\max} &= \frac{1}{8} Fl \\ &= \frac{1}{8} m a_{\max} l \\ &= W \sigma_{\max} \\ &\leq W [\sigma] \end{aligned} \quad (4-41)$$

where a_{\max} is the maximum detectable acceleration

and
$$W = \frac{bh^2}{6} \quad (4-42)$$

And then max acceleration can be calculated as:

$$\begin{aligned}
 a_{\max} &= \frac{W\sigma_{\max}}{\frac{1}{8}ml} \\
 &= \frac{4bh^2\sigma_{\max}}{3ml} \\
 &\leq \frac{4bh^2[\sigma]}{3ml}
 \end{aligned} \tag{4-43}$$

For a is the output value, the max metrical signal is just a_{\max} . It is a very important parameter to the choice of customers and users. On the other hand, the value of a_{\max} is relative to mass— m , so it is also a main standard of choosing an appropriate measurements for our CA.

4-4. Noise analysis and establishment of measurement

4-4-1. Noise analysis (Gabrielson, 1993)

There are many contributors to noise in an accelerometer. MEMS sensors are so small that the Brownian noise of the devices must be considered, while it is usually ignored in larger sensors. In micromechanical systems, the sensor noise floor is often set by the thermo-mechanical noise. This noise arises from the thermal motion of the atoms inside the structure and in the air (Brownian motion).

The Brownian noise equivalent acceleration of the system was given by Yazdi (1998):

$$a_e = \sqrt{4k_B TD} / gm \tag{4-44}$$

where k_B is Boltzmann's constant ($k_B = 1.38 \times 10^{-23} J / K(\text{joules / kelvin})$), T is

absolute temperature ($T = 0^{\circ}C$ or $T = 273K(kelvin)$) and D is damping coefficient.

The exact value of the damping coefficient D does not need to be computed and can be dominated with the quality factor, Q , of the system under harmonic excitation according the following formulation:

$$D = \sqrt{km} / Q \quad (4-45)$$

where k is the elastic coefficient of the system, m is the general mass. And we can get the value of the quality factor through the following formulation:

$$Q = d\sqrt{mk} / \mu A \quad (4-46)$$

where d is the gap between the mass and the substrate, and A is the area of horizontal cross-section of the mass (s), and $\mu = 18 \times 10^{-6} kg / m \cdot s$ is the viscosity of air at $20^{\circ}C$.

Substituting equations (4-45) and (4-46) into equation (4-44). The Brownian noise equivalent acceleration of the system is shown as:

$$a_e = \sqrt{4\mu k_B T A / dg^2 m^2} \quad (4-47)$$

4-4-2. Minimum detectable signal (Oosterbroek, 1999)

The minimum detectable signal (MDS) is a very useful parameter for the sensors. Knowledge of the MDS is also necessary when calculating the dynamic range or signal to noise ratio for a particular receiver configuration. The following treatment outlines a straightforward method to derive the MDS.

From the analyses above, we can get the thermal noise equivalent voltage spectral density as follow (Connor 1982):

$$N_0 = a_e S \quad (4-48)$$

where S is the sensitivity of sensor.

The bandwidth of the system is:

$$BW = \sqrt{k/m} / Q \quad (4-49)$$

Then substituting Q and BW into the equation above, the minimum detectable signal will be obtained:

$$\begin{aligned} MDS &= N_0 \times \sqrt{BW} / S \\ &= \sqrt{4k_b TDBW} / gm \\ &= \mu A / dg \times \sqrt{4k_b T / m^3} \end{aligned} \quad (4-50)$$

4-4-3. The establishment of measurement

4-4-3-1. Reference of existing product

As a MEMS pioneer, Analog Devices has held a leadership position as the industry's largest volume supplier of integrated MEMS accelerometers and gyroscopes. Anyway the analog is a famous brand in the field of sensors and actuators, and the types of their productions are also very many. They have mature technology at the same time.

And the diagram below shows us two different production's parameter. Those parameters will be the important gist of our accelerometer's design.

Part#	# of Axes	Range	Sensitivity	Sensitivity Accuracy (%)	Max Band Width (kHz)	Noise Density ($\mu\text{g}/\text{rtHz}$)	Supply Current (mA)
ADXL204	2	$\pm 1.7\text{g}$	620 mV/g	± 5	2.5	170	0.5
ADXL322	2	$\pm 2\text{g}$	420 mV/g	± 10	2.5	220	0.5

Table (4-2): Guideline of performance of analog products

So these two types of products are shown above are good samples and references for us to design our accelerometer. Further information about MEMS and sensor can be obtained from website (Analog Devices)

4-4-3-2. Establishment of measurement

By analyzing these parameters we can define a group of available measurement.

For the metrical precision is about 10^{-6} m, this group of measurements have been defined and shown below:

unit(μm)								
b	h	l	w	t	L	A	B	δ
50	30	600	300	30	300	50	50	30

Table (4-3): Measurements of structure

To express this group of measurements clearer, I use the figure below to show what these sizes denote:

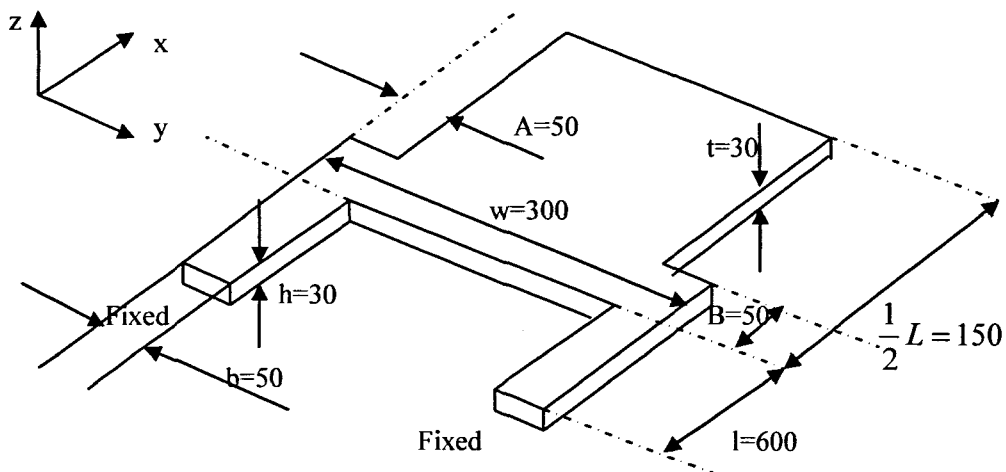


Figure (4-7): Measurement of structure

The material that we are going to use is silicon, and the density of silicon is:

$$\rho_{Si} = 2330 \text{ kg} / \text{m}^3 \quad (4-51)$$

And the volume of the central proof mass is:

$$\begin{aligned} V &= w \times t \times L - 2 \times A \times (300 - 2 \times B) \\ &= 300 \times 300 \times 30 - 2 \times 200 \times 50 \times 30 \\ &= 2.1 \times 10^6 \mu\text{m}^3 \\ &= 2.1 \times 10^{-18} \text{ m}^3 \end{aligned} \quad (4-52)$$

So the mass— m of the concentrative mass

$$\begin{aligned} m &= \rho V \\ &= 2.33 \times 10^{-15} \times 2.1 \times 10^6 \\ &= 4.893 \times 10^{-9} \text{ kg} \end{aligned} \quad (4-53)$$

And then the minimum detectable signal is:

$$\begin{aligned}
MDS &= \mu A / dg \times \sqrt{4k_B T / m^3} \\
&= \frac{(18 \times 10^{-6}) \times (7 \times 10^{-8})}{3 \times 10^{-5} \times 9.8} \times 2 \times \sqrt{\frac{(1.38 \times 10^{-23}) \times 273}{(4.893 \times 10^{-9})^3}} \\
&= 4.28575 \times 10^{-9} \times 1.79 \times 2 \times 10^2 \\
&= 1.5343 \times 10^{-6} \text{ m/s}^2
\end{aligned} \tag{4-54}$$

Note: the area of bottom plate is bigger than upper plate, so we use the area of the upper plate as the relative area between these two plates.

The result is in the range of 10^{-6} , so the measurement is basically appropriate. After this calculation, we can also calculate other effective parameters, such as sensitivity accuracy, max band range, voltage supply and noise density and so on.

4-5. Some necessary parameters' calculation

After the measurements were confirmed, we need to calculate some necessary parameters.

4-5-1. The formula of sensor

For $\Delta C = \frac{ml^3 \epsilon_0 s}{4Ebh^3 \delta_0^2} a$, we need to calculate the coefficient.

$$\begin{aligned}
\frac{ml^3 \epsilon_0 s}{4Ebh^3 \delta_0^2} &= \frac{4.893 \times 10^{-9} \times (6 \times 10^{-4})^3 \times 8.85 \times 10^{-12} \times 7 \times 10^{-8}}{4 \times 1.9 \times 10^{11} \times 5 \times 10^{-5} \times (3 \times 10^{-5})^3 \times (3 \times 10^{-5})^2} \\
&= \frac{65474.2116 \times 10^{-41}}{9234 \times 10^{-19}} \\
&= 7.0905 \times 10^{-22}
\end{aligned} \tag{4-55}$$

So finally:

$$\Delta C = 7.0905 \times 10^{-22} a \quad (4-56)$$

4-5-2. Sensitivity

The expression of sensitivity has been derived in front (equation (4-20)), it is:

$$S = \frac{ml^3 \varepsilon_0 s}{4Ebh^3 \delta_0^2} \quad (4-57)$$

Substituting each parameter, we have:

$$\begin{aligned} S &= \frac{4.893 \times 10^{-9} \times (6 \times 10^{-4})^3 \times 8.85 \times 10^{-12} \times 7 \times 10^{-8}}{4 \times 1.9 \times 10^{11} \times 5 \times 10^{-5} \times (3 \times 10^{-5})^3 \times (3 \times 10^{-5})^2} \\ &= \frac{65474.2116 \times 10^{-41}}{9234 \times 10^{-19}} \\ &= 7.0905 \times 10^{-22} F / g \end{aligned} \quad (4-58)$$

4-5-3. The max detectable acceleration

$$\begin{aligned} a_{\max} &\leq \frac{4bh^2 [\sigma]}{3ml} \\ &= \frac{4 \times 5 \times 10^{-5} \times 9 \times 10^{-10} \times 7 \times 10^9}{3 \times 4.893 \times 10^{-9} \times 6 \times 10^{-4}} \\ &= \frac{1260 \times 10^{-6}}{88.074 \times 10^{-13}} \\ &= 1.43 \times 10^8 m/s^2 \end{aligned} \quad (4-59)$$

4-5-4. The Brownian noise equivalent acceleration of the system

$$\begin{aligned}
a_e &= \sqrt{4\mu k_B TA / dg^2 m^2} \\
&= \sqrt{\frac{4 \times 18 \times 10^{-6} \times 1.38 \times 10^{-23} \times 273 \times 7 \times 10^{-8}}{3 \times 10^{-5} \times 96.04 \times 23.9414 \times 10^{-18}}} \\
&= \sqrt{\frac{189876.96 \times 10^{-37}}{6897.9962 \times 10^{-23}}} \\
&= 5.247 \times 10^{-7} \text{ m/s}^2
\end{aligned} \tag{4-60}$$

4-5-5. Thermal noise equivalent voltage spectral density (noise density)

$$\begin{aligned}
N_0 &= a_e S \\
&= 5.247 \times 10^{-7} \times 7.0905 \times 10^{-10} \\
&= 3.7204 \times 10^{-16} \text{ F/s}^2
\end{aligned} \tag{4-61}$$

4-5-6. The bandwidth of the system

Substituting quality factor Q into this (4-62) and the elastic coefficient k will be vanished:

$$\begin{aligned}
BW &= \sqrt{k/m} / Q \\
&= \frac{\sqrt{k/m}}{d\sqrt{mk} / \mu A} \\
&= \frac{\mu A}{md} \\
&= \frac{18 \times 10^{-6} \times 7 \times 10^{-8}}{4.893 \times 10^{-9} \times 3 \times 10^{-5}} \\
&= 8.5837(1/s)
\end{aligned} \tag{4-62}$$

4-5-7. The minimum detectable signal

We have already calculated the minimum detectable signal when we selected measurements.

$$\begin{aligned}
 MDS &= \mu A / dg \times \sqrt{4k_B T / m^3} \\
 &= 1.5343 \times 10^{-6} \text{ m/s}^2
 \end{aligned}
 \tag{4-63}$$

4-5-7-1. Why minimum detectable signal (Millitech, 2004)

There are a wide range of applications for which it is desirable or necessary to know the minimum power level at which a system receiver can detect an incoming signal. Because the minimum detectable signal (MDS) also pertains to the noise floor of system receiver, this is of particular import when the received power level may be close to the MDS. Knowledge of the MDS is also necessary when calculating the dynamic range or signal to noise ratio for a particular receiver configuration. The following treatment outlines a straightforward method to derive the MDS.

4-5-7-2. White noise (Millitech, 2004)

White noise is the blanket noise, containing a uniform power density per unit frequency interval, which is present in all electrical system. It can be shown that the noise power contained in an millimeter-wave receiver is given by Boltzman's Law, i.e.,

$$\text{NoisePower} = kTb$$

$$k = \text{Constant}$$

$$T = \text{Absolute Temperature (Kelvin)}$$

$$b = \text{Measurement Bandwidth}$$

In 1 Hz of measurement bandwidth, and at room temperature (293 Kelvin), the noise power contribution to the system receiver by white noise is:

$$kTb = -174 \text{ dBm.}$$

4-5-8. Elastic coefficient and resonant frequency

The equation (4-22) can be written as:

$$\omega_n = \sqrt{\frac{k}{m}} = \sqrt{\frac{ma}{\Delta\delta}} = \sqrt{\frac{a}{\Delta\delta}} \quad (4-64)$$

And ulteriorly, from equation (4-8), $\Delta\delta = \frac{mal^3}{4Eb^3}$, so the frequency of system can be

written as:
$$\omega_n = \sqrt{\frac{4Eb^3}{ml^3}} \quad (4-65)$$

So the value of resonant frequency will be:

$$\begin{aligned} \omega_n &= \sqrt{\frac{4 \times 1.9 \times 10^{11} \times 5 \times 10^{-5} \times (3 \times 10^{-5})^3}{4.893 \times 10^{-9} \times (6 \times 10^{-4})^3}} \\ &= \sqrt{\frac{1026 \times 10^{-9}}{1056.888 \times 10^{-21}}} \\ &= 0.9853 \times 10^6 \text{ Hz} \end{aligned} \quad (4-66)$$

4-6. The introduction of circuit diagram of the accelerometer

We are just designing the inner structure of the accelerometer and the circuit diagram of all capacitive accelerometer is approximately same. So we only do an ordinary introduction of circuit here.

4-6-1. The typical circuit sample of CA

First of all, we introduce a typical circuit diagram. Figure (4-8) shows a block diagram for a typical capacitive accelerometer: simply consisting of a voltage source, a capacitive sensing element, and a signal conditioning output portion. More information about CA can be obtained from the website (CAPACITIVE

ACCELEROMETERS (b))

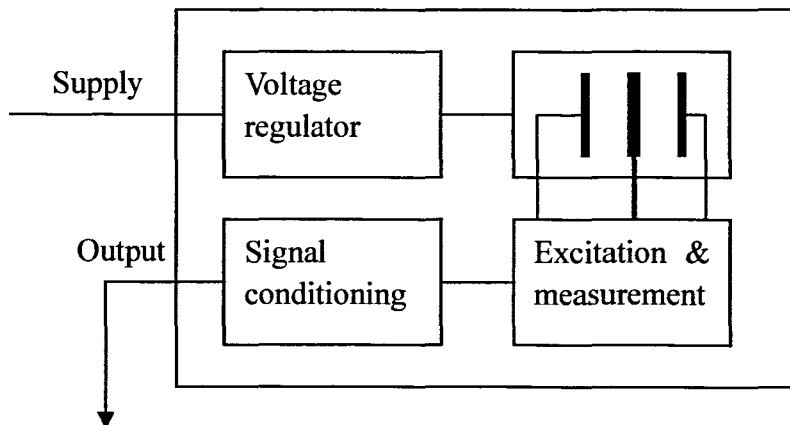


Figure (4-8): A typical circuit diagram for capacitive accelerometers

This is a real product picture (Figure (4-9)) which can show us the elements inside clearer:

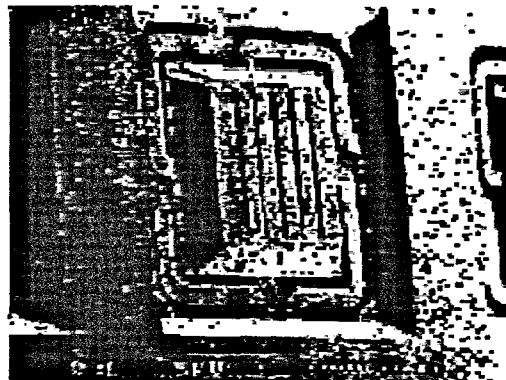


Figure (4-9): Photo of Silicon Microstructures' 7130 Capacitive Micro machined Accelerometer

This is an example that is shown in Figure (4-9); an etched silicon wafer with proof mass and connecting beams.

4-6-2. The introduction of existing product's circuit

We'll introduce some existing sensors' circuit diagram of analog product; they'll be shown below by some figures:

4-6-2-1. One axis sensor:

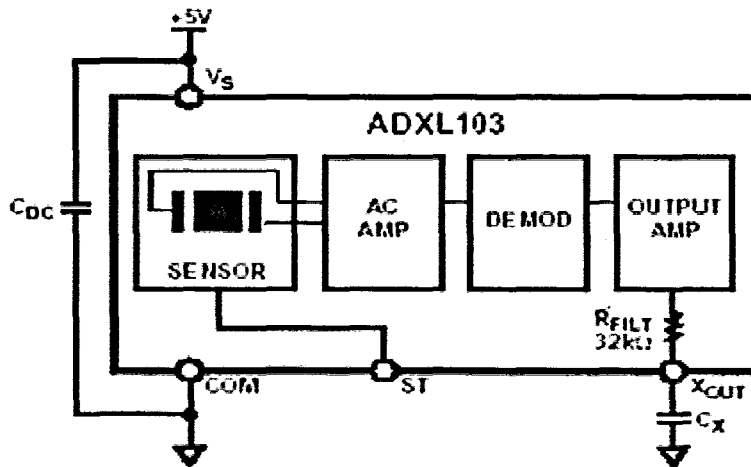


Figure (4-10): The two axes sensor

4-6-2-2. Two axes sensor:

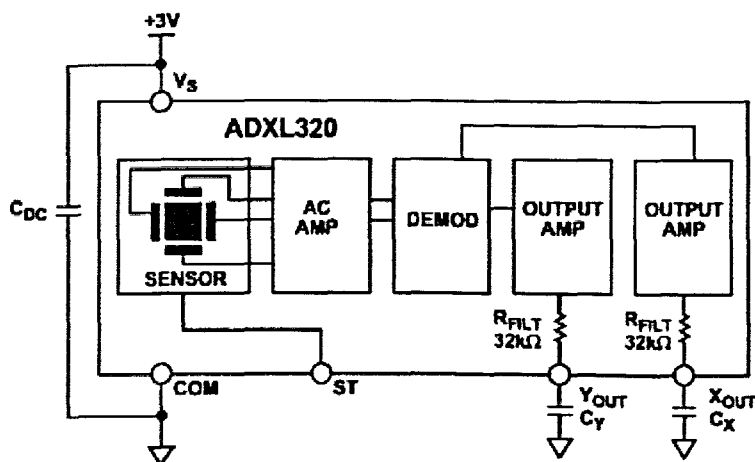


Figure (4-11): The one axis sensor

For the detail, please check the website (Analog Devices)

4-6-2-3. Theory of operation (Analog Devices)

The ADXL103/ADXL203 are complete acceleration measurement systems on a single monolithic IC. The ADXL103 is a single axis accelerometer, while the ADXL203 is a dual axis accelerometer. Both parts contain a polysilicon surface-micromachined sensor and signal conditioning circuitry to implement an open-loop acceleration measurement architecture. The output signals are analog voltages proportional to acceleration. The ADXL103/ADXL203 are capable of measuring both positive and negative accelerations to at least $\pm 1.7g$. The accelerometer can measure static acceleration forces such as gravity, allowing it to be used as a tilt sensor. The sensor is a surface-micromachined polysilicon structure built on top of the silicon wafer. Polysilicon springs suspend the structure over the surface of the wafer and provide a resistance against acceleration forces. Deflection of the structure is measured using a differential capacitor that consists of independent fixed plates and plates attached to the moving mass. The fixed plates are driven by 180° out-of-phase square waves. Acceleration will deflect the beam and unbalance the differential capacitor, resulting in an output square wave whose amplitude is proportional to acceleration. Phase sensitive demodulation techniques are then used to rectify the signal and determine the direction of the acceleration. The output of the demodulator is amplified and brought off-chip through a 32 k Ω resistor. At this point, the user can set the signal bandwidth of the device by adding a capacitor. This filtering improves measurement resolution and helps prevent aliasing.

4-7. Summary

We got the basic math model $\Delta C = \frac{ml^3 \epsilon_0 s}{4Ebh^3 \delta_0^2} a$ through static analysis. This is just

the essential working principle of our CA. After the dynamic analysis, we find the dynamic math model:

$$\Delta C = \frac{2[(2\pi f_n)^2 - (2\pi f)^2] ml^3 \varepsilon_0 s}{4Eb^3 \delta_0^2 V_a^2 mgz(l) [\sin 2\pi ft - (f/f_n)] \times [\sin kx - \sinh kx + S(\cos kx - \cosh kx)]} a$$

This equation can be used to calculate transient value of change of capacitance. The stress analysis provide a approach of getting the maximum acceleration

$$a_{\max} \leq \frac{4bh^2[\sigma]}{3ml} = 1.43 \times 10^8 \text{ m/s}^2$$

This is the metrical precision which will be the important measure to the accelerometer's performance. The primary task of this chapter is to improve the performance and capabilities of our CA. See Table (4-4) that the frequency and sensitivity are high, the detectable signal (acceleration) range is wide, the noise disturbance is little, and so we can say that the CA with simple crab-structure is developed.

sensitivity	$7.0905 \times 10^{-22} \text{ F/m}$
The max detectable acceleration	$1.43 \times 10^8 \text{ m/s}^2$
The minimum detectable signal	$1.5343 \times 10^{-6} \text{ Js/m}$
noise density	$3.7204 \times 10^{-16} \text{ F/s}^2$
bandwidth	$8.5837(1/s)$
resonant frequency	$0.9853 \times 10^6 \text{ Hz}$

Table (4-4): the important parameters of our CA

Chapter 5

Analysis by CoventorWare

5-1. Introduction of CoventorWare

CoventorWare supports both system-level and physical approaches to designing MEMS and microfluidic devices. The system-level approach involves use of behavioral model libraries with a high-speed system simulator. The system-level design can be used to generate a 2-D layout for physical level verification. The physical approach starts with a 2-D layout and involves building a 3-D model, generating a mesh, and simulating using FEM or BEM solvers. Custom reduced-order macromodels can be extracted for use in system simulations. Finally, the verified 2-D layout can be transferred to a foundry for fabrication. CoventorWare has numerous options, including design libraries and a variety of 3-D physics solvers. Various entry and exit points allow import and export of files from and to other third-party software, for example, the software by the name of Solid Edge, MATLAB, Solid Works and EdgeCAM etc.

CoventorWare can be described as a circularly connected series of modules. Designs may begin at different places in this flow, depending on whether users choose to design at the system or physical level.

There is a flow map which can show us how this software works.

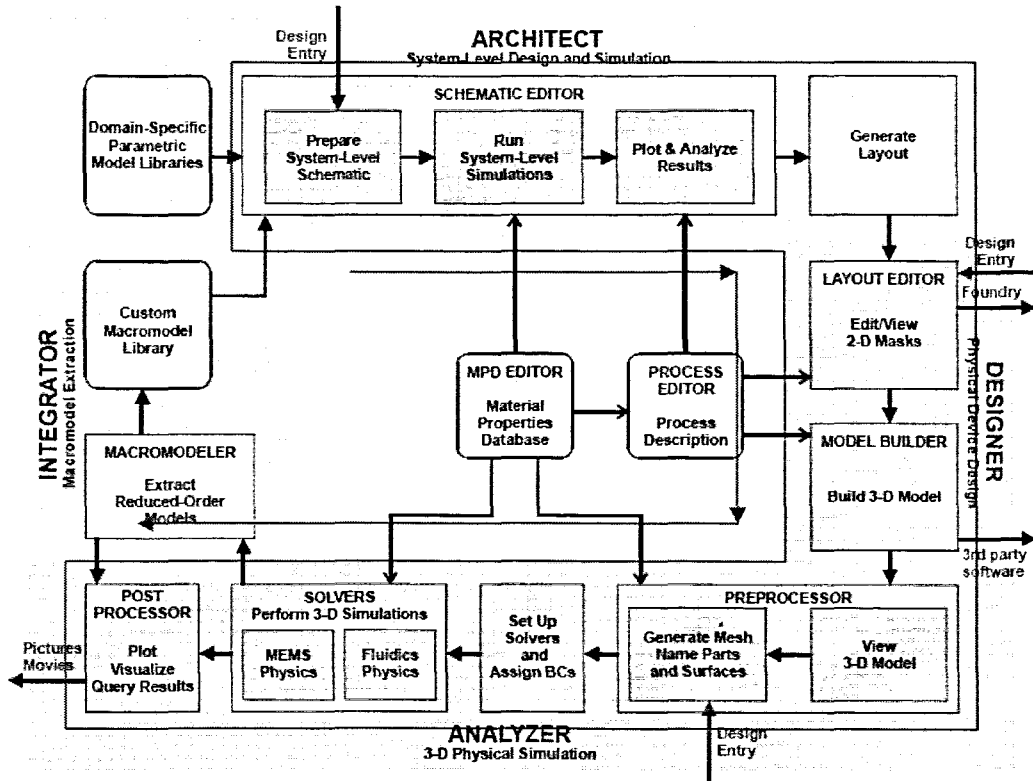


Figure (5-1): the flow map of CoventorWare working

- **System-level design**

Starts with a schematic containing behavioral model and uses a system simulation to solve a coupled set of ODEs.

- **System simulation**

Takes schematic as input and performs high-speed DC, AC, and transient simulations.

- **Physical device design**

Starts with a 2-D layout of device and uses FEM/BEM to simulate 3-D physical effects.

- **3-D physics simulation**

Use 3-D finite element (FEM) or boundary element (BEM) method to solve equations at each element node of a 3-D mesh.

Next, our work will be carried out along with the steps which are enclosed with red rectangles (Figure (5-1)).

5-2. Creation of architect model

The difference between the steps in this chapter and the steps in chapter 2 is that we make an architect model instead of drawing a 2-D layout, and the architect model can generate a 2-D layout and 3-D model automatically. The purpose of doing so is to do more complex and wider analyses which base on the architect model. This should be a necessary step of our work in this chapter.

Architect design is a system-level design; it uses a “structured custom” approach to MEMS device development. The block diagram below outlines the steps. The shaded boxes represent architect functionality.

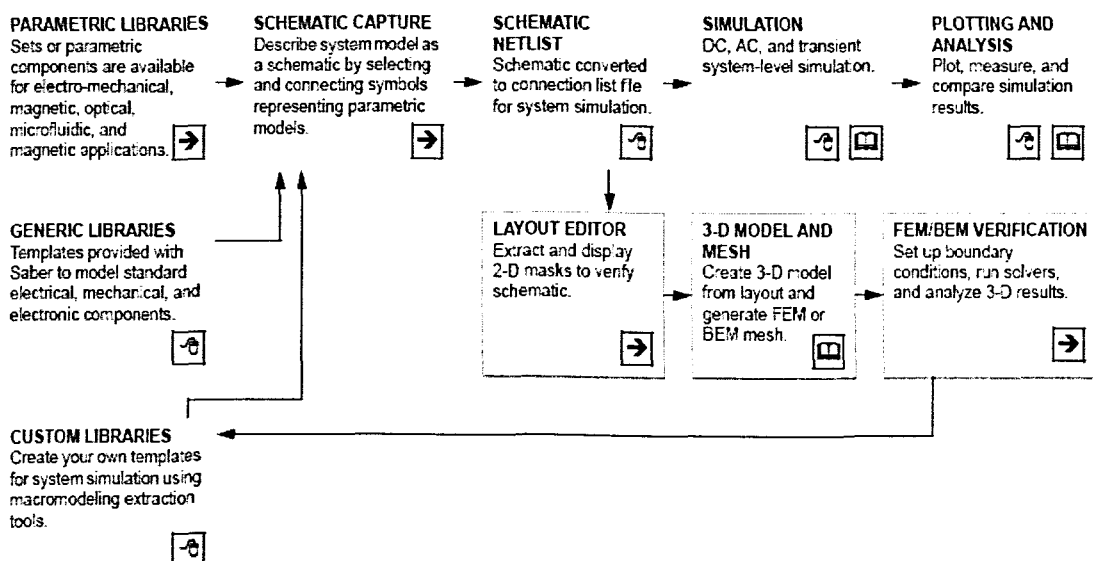


Figure (5-2): the block diagram of architect work

We can see from this block diagram that we must create a schematic if we want to do the simulation and plotting and analysis. At the same time, we can also generate the 2-D and 3-D model to do FEM (finite element method) analysis.

Next, we skip the steps of schematic creation and show the architect model we have done by using Saber (the tool for creating architect model) directly.

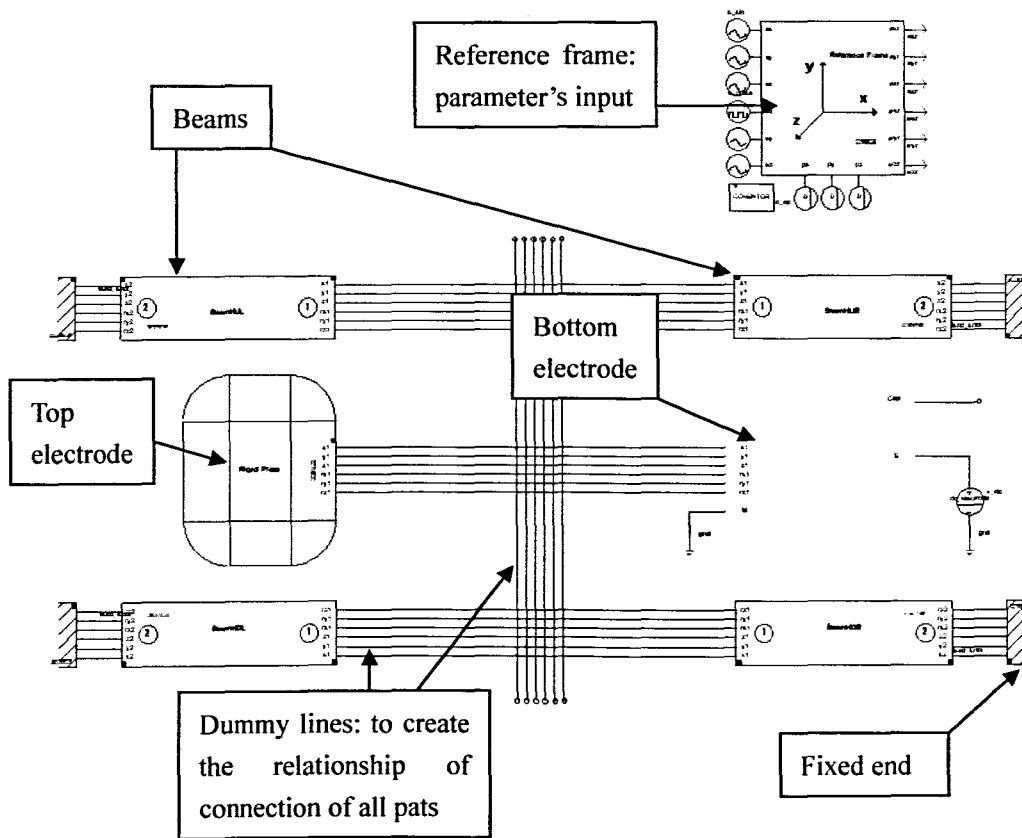


Figure (5-3): the architect model of our accelerometer

The figure shows us clearly the function and name of each part. All parts come from the library component in CoventorWare. After drawing these parts we must input the feature, such as length, width, area etc, of them and create the relationship of connection between every two parts.

5-3. Generate 2-D layout and 3-D model

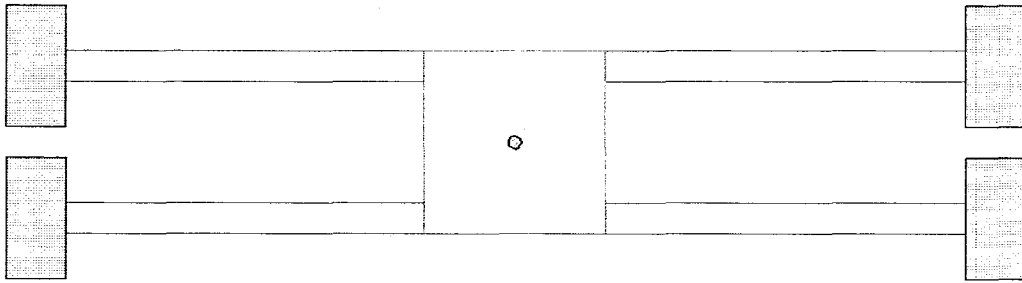


Figure (5-4): 2-D layout generated by architect model

During the course of schematic creation, many parameters have been entered in the properties window for each component. The Layout Editor reads the netlist files generated by Architect. Through the use of built-in layout generators, the 2-D layout for the accelerometer design is constructed.

When you start preprocessor, the system of architect will generate the 3-D model.

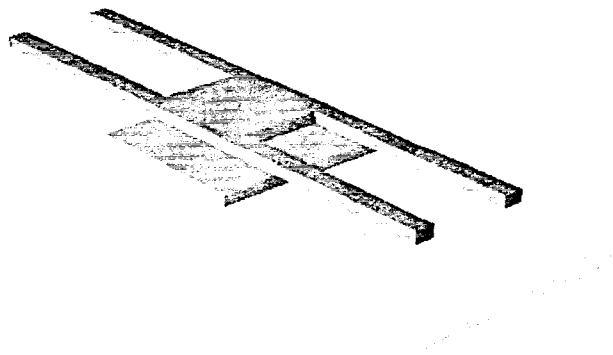


Figure (5-5): 3-D model

That is mainly for the analysis of FEM. We'll introduce it in latter section.

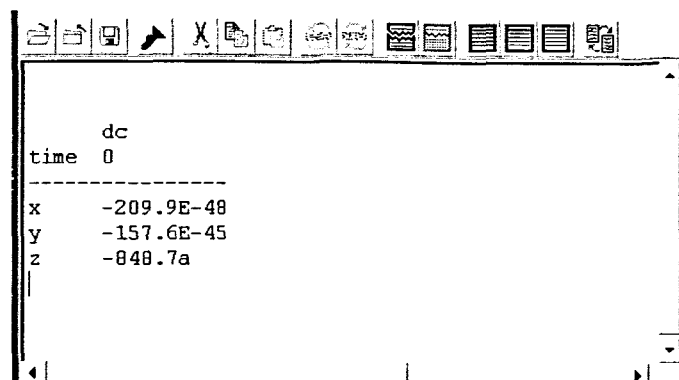
Note: the 3-D model here looks different from the one we have used in chapter 2. The main reason is that these two 3-D models are generated by different sources. The first one comes from the 2-D layout that we draw by hand directly; nevertheless the second one is generated by normative parts in Architect library, and these normal parts have already been designed, the shape of rigid plate (concentrative mass) cannot be changed. But the effect of FEM analysis should be same basically because we input same quantity to the mass.

5-4. Architect accelerometer performance analysis

Architect can simulate the behavior of the accelerometer. The simulation results can then be used to optimize the performance of the device.

5-4-1. DC operation point analysis

A DC operating point analysis provides the initial solution for all other analyses. DC analysis is a two-step verification for the completeness of the schematic. First, before performing the DC operation point analysis, Saber generates a netlist. If some required attributes are missing or if some design variables have no numerical value, Saber will fail to read this netlist. If this happens, an error message should explain which component is incorrect and DC analysis results give a fast overview of attribute correctness: X, Y and Z coordinate values.



The image shows a screenshot of a software window with a toolbar at the top. The window displays the following text:

```
dc
time 0
-----
x    -209.9E-48
y    -157.6E-45
z    -848.7a
```

Table (5-1): coordinate values for X, Y and Z axes

5-4-2. DC transfer (sweep) analysis

This analysis can show us the change of voltage along with the vibration.

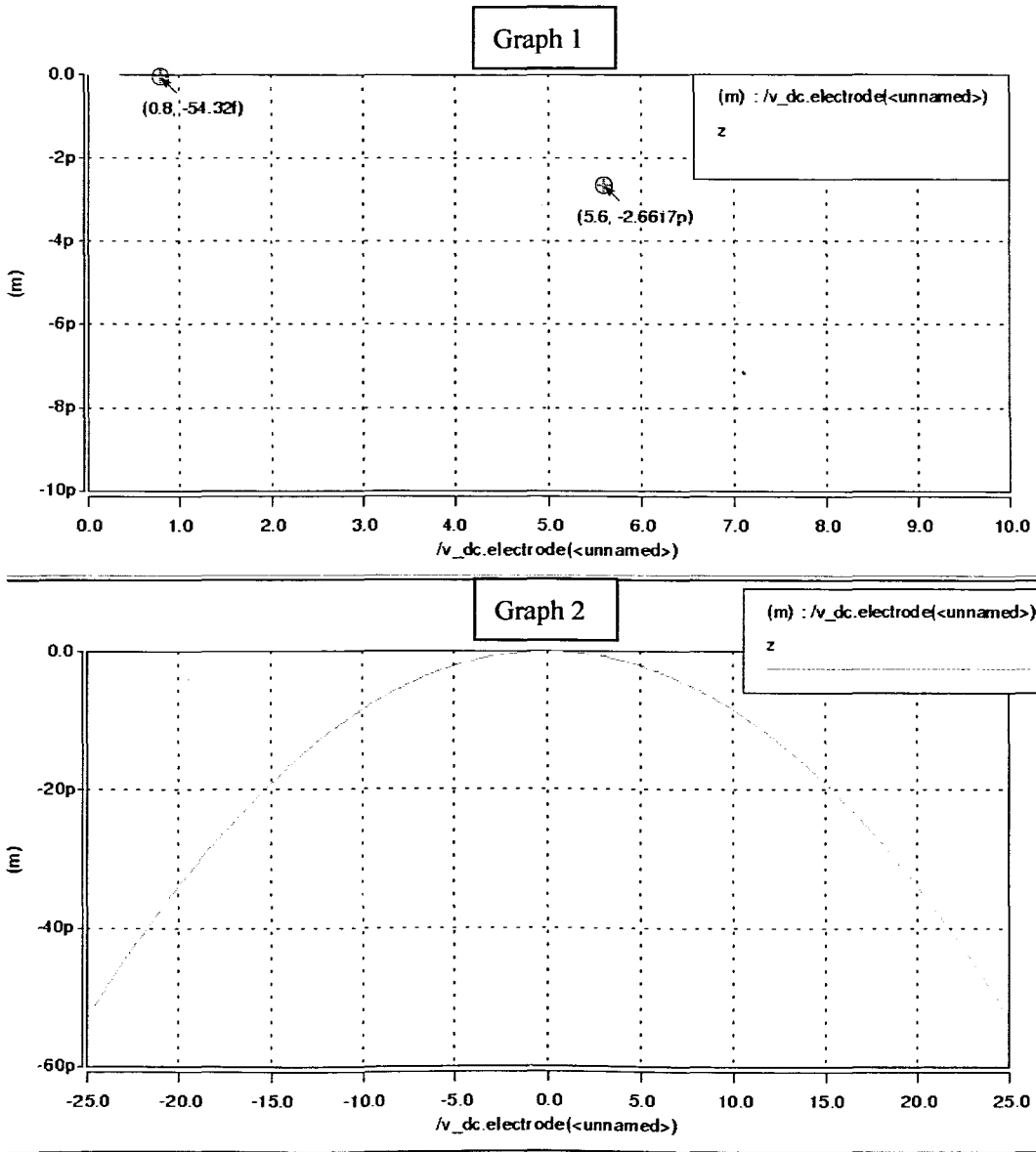


Figure (5-6): DC transfer (sweep) analysis

Graph 1 and graph 2 show the change of voltage in different region. Graph 1 shows single vibration direction and graph 2 shows two vibration directions.

5-4-3. Small signal AC analysis

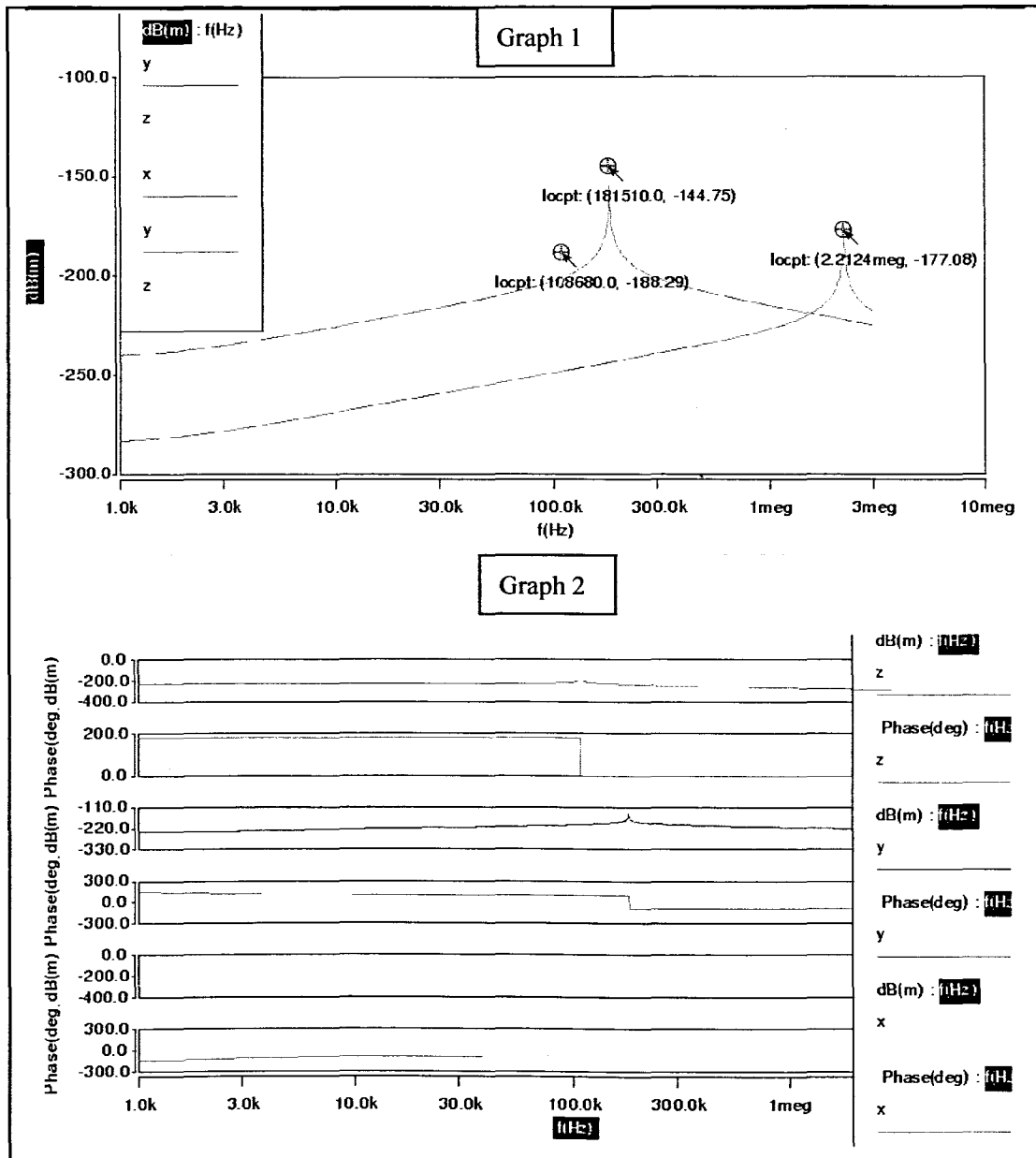


Figure (5-7): the resonant frequencies of three axes

Graph 1 shows three resonant frequencies of axes X, Y and Z. We can check the peak signal points of each direction from it. Graph 2 plots the frequencies in different modes.

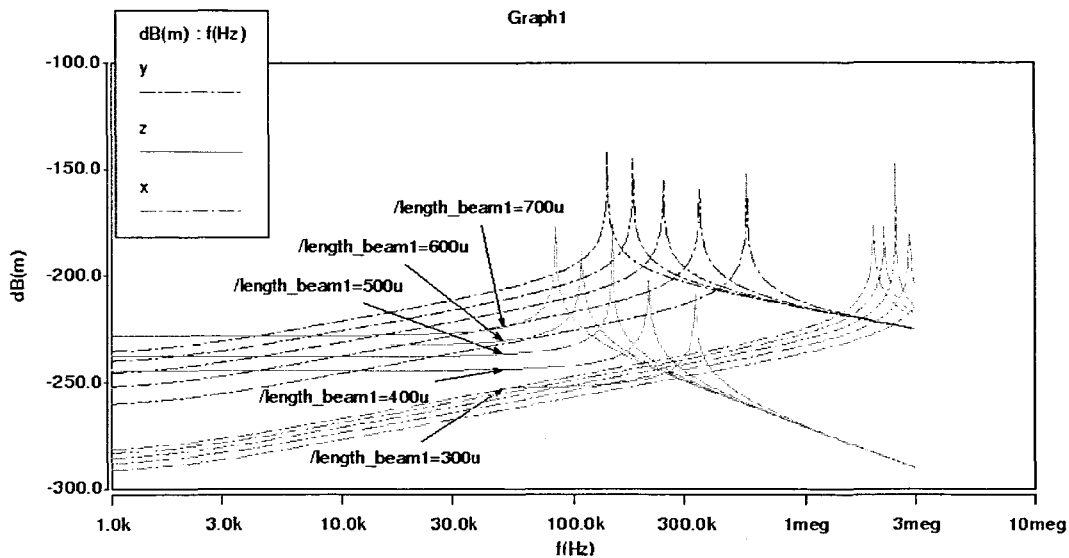


Figure (5-8): resonant frequencies of varying beam length

We can see that y and z mode resonant frequencies decrease while the x mode frequency remains almost the same. The relative position of the y and z mode resonant frequencies change and the resonance matching occurs around $\text{length_beam1}=500 \mu\text{m}$. For good cross talk performance, the x mode resonant frequency should be as far as possible from the y and z mode resonant frequencies, but these last two frequencies should not be too low.

To our structure, the resonant frequency of x mode is far enough from y and z mode resonant frequencies (from 3000k (Hz) to 3meg (Hz)) and y and z frequencies are not too low (y: 150k (Hz)-800k (Hz), z: 80k (Hz)-300k (Hz)).

5-4-4. Sensitivity analysis

The sensitivity analysis is an alternate and very effective method to study the impact of design parameters on a given performance parameter such as resonance frequency, dc point displacement, transient amplitude etc. With a sensitivity analysis the sensitivity of a parameter is calculated by a measurement-based perturbation method. A specified parameter p is perturbed from its nominal value, and the effect on a

specified performance measure F for the design is determined as shown below:

$$sensitivity = \frac{\delta F}{\delta p}$$

To provide meaningful comparisons, the results are usually normalized:

$$sensitivity = (\Delta F / F) / (\Delta p / p) \Rightarrow \Delta F = sensitivity \cdot F \cdot (\Delta p / p)$$

where p the nominal value of the perturbed parameter
 Δp the amount by which the parameter is perturbed
 F the nominal value of the performance measure
 ΔF the amount by which the performance measure changes in response to the parameter perturbation

Note: the sensitivity here is different with the sensitivity that we have introduced and calculated in frontal chapters.

```
ac (fbegin 42k,fend 45k,increment linear,npoints 1000,siglist /x/y/z
meas maximum (cnames y,pfin pml_gyro.ac,ytrans mag
```

Sensitivity Report Options

```
Minimum sensitivity magnitude to report: 0
Report sorted by: Value
Sensitivity normalization: Normalized
Normalization threshold: 100E-15
```

Sensitivity of Maximum of MAG(y) in pfile pml_gyro.ac

Nominal Value = 24.486p

Instance	Part Type	Parameter Name	Nominal Value	Sensitivity	Bar-chart
-	-	length_beam1	600u	3.67	-----
-	-	width_beam1	50u	-2.72	-----
-	-	poly_layer->elastic	169g	-1.05	---
-	-	poly_layer->h	30u	0.158	.

Table (5-2): sensitivity report

The sensitivities of length_beam1, width_beam1, poly_layer->elastic, poly_layer->h has already been shown in the table (5-2).

5-4-5. Monte Carlo analysis

The Monte Carlo analysis can show us the relative distribution of the resonance frequency of the accelerometer's driving mode.

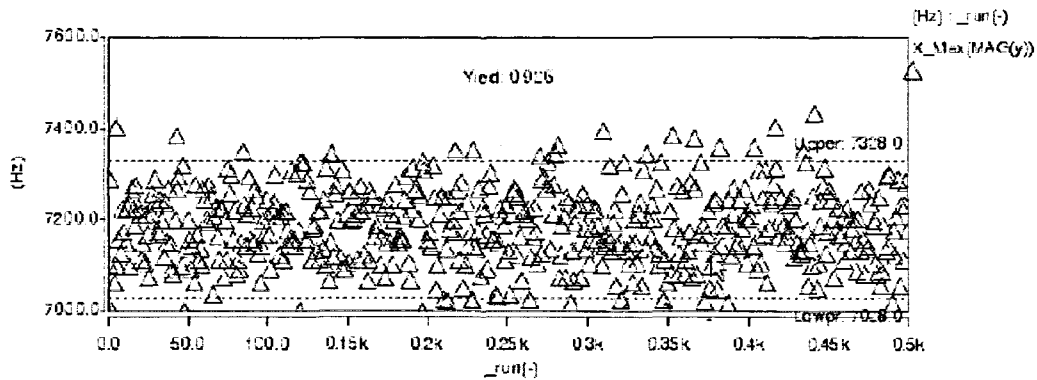


Figure (5-9): result of Monte Carlo analysis

The appearance of the graphs in figure (5-9) will vary from run to run due to the statistical nature of the Monte Carlo analysis. Needless to say, the accuracy of statistical analysis strongly depends on the number of sample points taken. The bigger the number of runs in the Monte Carlo analysis the more accurate and reproducible are the results.

5-4-6. Impact of plate curvature

MEMS structures are typically deformed by surface stress caused by the manufacturing process. The common architect parameter curvature can be used to study the impact of rigid plate curvature on the device performance. The curvature parameter is available in the rigid plate, beam, and electrode components.

With the six sub-parameters of the component parameter curvature (x_0 , y_0 , c_1 , c_2 , c_3 , c_4 , c_5), the user can specify a parabolic curvature surface of a rigid plate in the reference coordinate system

$$z = f(x, y) = c_1(x - x_0)^2 + c_2(y - y_0)^2 + c_3(x - x_0)(y - y_0) + c_4(x - x_0) + c_5(y - y_0)$$

The constants of curvature profile are usually derived from interferometric measurements of the released structure or by measuring the vertical position of designated points such as plate corners or the plate center. Alternatively, if the material stress gradients of the fabrication process are well known, plate bending can be analyzed in a FEM verification step using MemMech.

For the following simulation we assume a symmetric bending of the plate with its local minimum in the center of the plate. We therefore only need to specify the polynomial constants c_1 , and c_2 of the equation above. We will start by specifying a fixed curvature by setting the design variable to $c=1$. The simulated parabolic curvature surface of a rigid plate will consequently be set to:

$$z = f(x, y) = x^2 + y^2$$

From the DC operating point analysis (Table (5-3)), we find that the applied curvature causes a central knot (center of the plate) to move 108.4nm in negative z direction which will make an important effect on the sensitivity of the device.

Fabrication defects like plate curvature and beam side wall angles are often the cause of mismatches between measured and simulated data. Furthermore, unsymmetrical plate curvature (mismatch between the plate center and the local minimum x_0, y_0 of the assumed parabolic shape) are often the source of unexpected device behavior like staggering motions and an increased cross sensitivity.

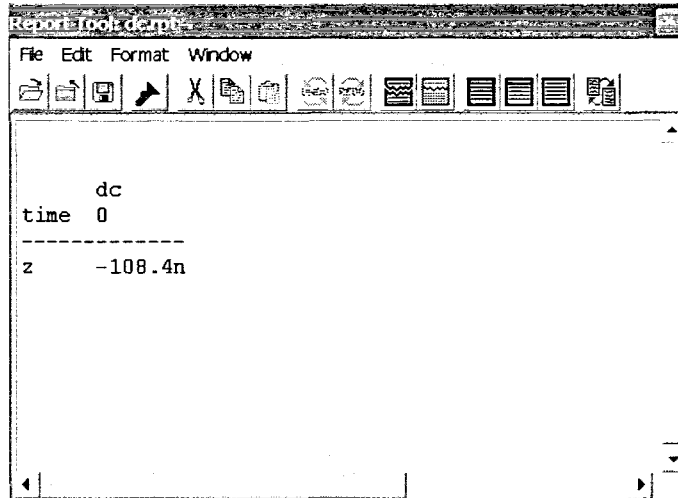


Table (5-3): operating point report of plate curvature

The Saber vary analysis is a convenient way to investigate the reasons for a mismatch (e.g. plate curvature, staggering motion) between measured data and ideal device behavior.

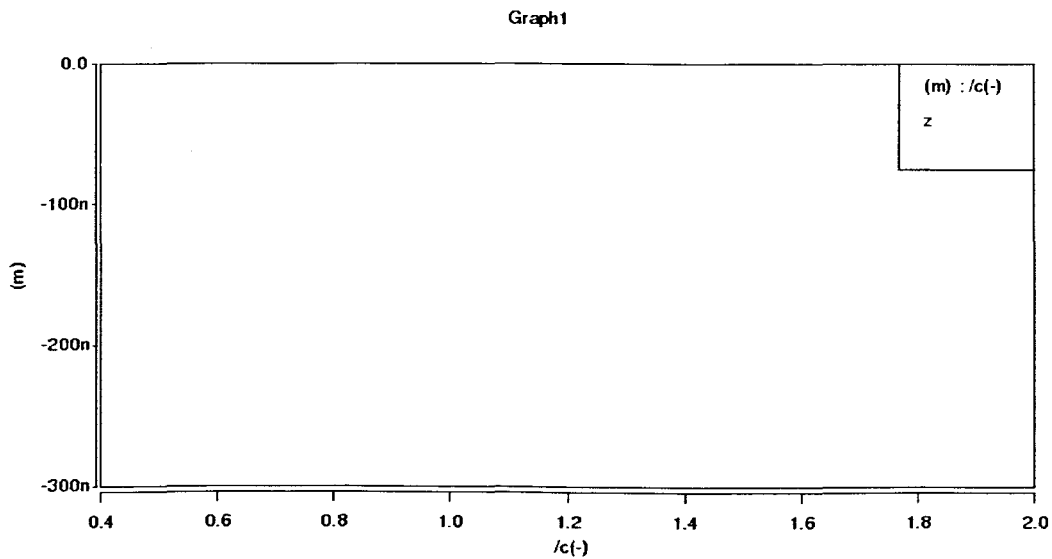


Figure (5-10): result of vary analysis

In similar fashion, the vary analysis can be used to investigate the impact of plate curvature on the resonance frequencies or even on the transient performance. For our example the curvature effect on the first resonance frequencies is very small.

5-4-7. FEM analysis

The purpose of the following procedures is to compare the system model results with FEM analysis results for resonance frequencies. A modal analysis will be conducted using the MemMech solver.

First of all, we need to create the mesh model from the 3-D model.

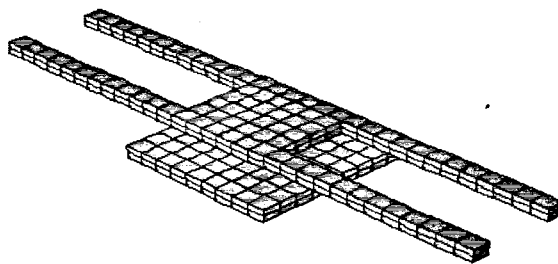


Figure (5-11): 3-D mesh mode for doing FEM analysis

Next, modal analysis is performed on the accelerometer. MemMech solves an eigenvalue problem to find the natural frequencies and mode shapes of the structure.

modeDomain	Frequency	Generalized Mass	Damping
1	1.044086E05	6.919874E-09	0.0
2	1.865338E05	7.508392E-09	0.0
3	2.676600E05	3.705959E-09	0.0
4	3.335556E05	4.657062E-09	0.0
5	5.670923E05	3.572520E-09	0.0
6	6.711327E05	3.911652E-09	0.0

Close

Table (5-4): frequency results

5-5. Summary to the result of analysis

The primary aim of this chapter is to verify our CA's performance and the result calculated in chapter 4 through CoventorWare analysis. By creating the architect model, we have done seven types of analyses; they are from DC point analysis to FEM analysis.

The coordinate values for X, Y and Z axes have been calculated by doing DC point analysis. The relationship between vibration position and voltage was linear in DC transfer analysis, and the value change of voltage is acceptable. The small signal AC analysis shows us the graphical interfaces of frequencies. The frequencies shown in FEM analysis is very close to our calculation results. The discrepancy between them is primarily led by the difference of calculation means. Dichotomy is used by computer instead of common way we used. The Monte Carlo outputs more intuitionistic figure which can show us the distribution of frequencies further. The impact of plate curvature has been analyzed by DC point and Vary analysis. The outcome indicates that the effect of plate curvature is small enough to be ignored.

Chapter 6

Conclusions and Recommendations

6-1. Summary

In this paper, we are trying to design a better structure with good stability, high working level and to make it more efficient and convenient for making. We also consider as more as possible to reduce its cost. On the other hand, the purpose of improving this capacitive accelerometer's performance is very important too. The three objectives have been clarified in front in chapter 1.

- Design a practical structure for this capacitive accelerometer which is also convenient for making
- Develop its working performance and capability on the basis of reducing cost and clarify pivotal definitions and issues within the whole course of design
- Simulate the working situation and analyze the characters of this crab-shape accelerometer to verify its capability

On the basis of reading plenty of articles and literatures, we have designed our own CA structure—crab-structure, which structure can meet the first project, in chapter 3. The working performance of this crab-shape CA has been developed in chapter 4 by referencing some existing products and by doing static and dynamic analysis. The necessary parameters for measuring this CA's stand or fall have already been calculated too. Table (6-1) can show us the value of those parameters clearly. In chapter 5, we used the CoventorWare to verify our CA's working capabilities, and

these capabilities were analyzed and discussed as well.

Basically, we can say that our objectives have been accomplished in those five chapters respectively.

6-2. Conclusion

Parameters \ CAs	Our crab-shape CA	Surface Micromachined CA With Closed-Loop Feedback (Mutlu, 1997)	z-axis accelerometer (chapter 3, 3-4)	Analog product (ADXL204)
sensitivity	$7.1 \times 10^{-22} \text{ F/g}$	1.3 fF/g	0.75mv/g	620 mV/g
noise density	$3.72 \times 10^{16} \text{ F/s}^2$	---	0.6mg/rtHz	170 ($\mu\text{g/rtHz}$)
bandwidth	8.5837Hz	---	---	2.5kHz
The minimum detectable signal	$1.53 \times 10^{-6} \text{ m/s}^2$ ($1.56 \times 10^4 \text{ mg}$)	0.077mg	---	---
resonant frequency	$0.985 \times 10^6 \text{ Hz}$	5836 Hz	10.1kHz	---

Table (6-1): comparison of parameters

By contrast of following parameters with several existing CA's design and product in

Table (6-1), it is not difficult to draw a conclusion that our CA is working at a better condition than other types. We can also say that the CA we designed can be used for higher level and more precise detection, such as the control and guide of navigate missile. Anyway, the sensitivity (7.1×10^{-22} F/g) and the resonant frequency (0.985×10^6 Hz) of our CA are much higher than other samples, and the noise density (noise disturbance) is very little (3.72×10^{-16} F/s²).

On the other hand, the minimum detectable signal is also smaller than other ones. It means that our CA can detect smaller acceleration which can not be detected by other accelerometers. So our CA can be used for exacter detection in some fields.

6-3. Recommendations for the future

The developing current of contemporaneity sensor is being small, with high accuracy, precision and wider measurement range. So anyway, the techniques of some kinds of micro-sensors still need to be developed no matter the structure, material, even the sensing principle of the micro-sensors. I think the main direction of sensor technology improvement should be about the development of material and structure. On one hand, a kind of good quality material may promote a global revolution of technique in many fatal fields, not to speak of sensor field. On the other hand, a more efficient and practical structure can also bring benefit to development of micro-sensors.

In addition, the accelerometers (acceleration sensors) are being used in many fields and the technology of accelerometer is going to be perfect increasingly. But some problems of CA are still waiting for being solved more perfectly, for instance the disturbance of parasitic capacitance and the effect of electrostatic force.

There are still many kinds of sensors that don't have developing technique. So we need to try to develop these existing types of sensors' technique, such as liquid sensor,

gas sensor, and smell sensor and so on. We still need to invent new type of sensor for using in wider vocations when we are trying to extend the application range of these old types of sensors.

References

Analog Devices [online]. Available from:

<http://www.analog.com>

Bernstein, J., Miller, R., Kelley, W., Ward, P., 1999, Low-noise MEMS Vibration Sensor for Geophysical Applications, *Journal of MEMS* 8, 433-437

Berter, T., Kubler, J. M., Cuhat, D., 1993, Kapazitiver Miniatursensor zur Messung nieder-frequenter Beschleunigung, KISTLER Instruments AG

BOOKRAGS-ACCELEROMETER. Bookrags-Accelerometer [online]. Available from:

<http://www.bookrags.com/sciences/sciencehistory/accelerometer-woi.html>

Burger, J.F., Holland, H.J., Brake, H.J.M., Rogalla, H., Fast gas gap heat switch for a microcooler, Presented at the 10th International Cryocooler Conference, May 26-28 (1998) Monterey California.

CAPACITIVE ACCELEROMETERS (a). Capacitive accelerometers [online].

Available from:

<http://xenia.media.mit.edu/~verp/projects/smartpen/node17.html#secsecondorderss>

CAPACITIVE ACCELEROMETERS (b). Capacitive accelerometers [online].

Available from:

<http://xenia.media.mit.edu/~verp/projects/smartpen/node38.html>

Connolly, T., *Variable Capacitance Accelerometers: Design and Applications*, 1995,

Silicon Products Endevco Corporation 30700 Rancho Viejo Rd. San Juan Capistrano
CA 92675 USA

Connor, F.R., Noise, Second Edition, ISBN 0 7131 3459 3, 1982

Doescher, J., 1999, A High performance Surface Micromachined Accelerometer,
Analog Devices Inc.

Elwenspoek, M., and Wiegerink, R., Mechanical microsensors, Springer Verlag,
Heidelberg, to be published in 2000.

Gabrielson, T., Mechanical-thermal noise in micromachined acoustic and vibration
sensors, IEEE Trans. Elect. Dev., Vol-40, 1993, pp903-909.

Gabrielson, T.B., May 1993, Mechanical-thermal noise in micromachined acoustic
and vibration sensors, IEEE Trans, Electron. Devices, Vol. 40:903-909.

Garry, T., Xie, H. K., and Fedder, K., A cmos z-axis capacitive accelerometer with
comb-finger sensing, 2001, the Robotics Institute Carnegie Mellon University.

Hutyra, M., 1994, Monolytic accelerometer ADXL50, Automatizace 37, pp.225-227

Kloek B., Piezoresistive sensors, in: Sensors, Vol 7, ed. Göpel, W., Hesse, J., and
Zemel, J.N., VHC Verlagsgesellschaft, Weinheim, Germany, 1994, pp.145 - 172.

Liu, C., Barzilai, A., Reynolds, J., Partridge, A., Kenny, T., Grade, J., Rockstad, H.,
Characterization of a high-sensitivity micromachined tunneling accelerometer with
micro-g resolution, Micro, J., Elect. Mech. Syst., Vol-7, 1998, pg 235-244.

Madou, M., Winter 2005, BIOMEMS Class I-Introduction: From MEMS to BIOMEMS/Definitions

McCallion, H., *Vibration of Linear Mechanical Systems*, Longman Group, London, 1973, p. 103

McCord, M.A., Dana, A., and Pease, R.F.W., The micromechanical tunnelling transistor, *Micromech. Microeng., J.* Vol-8, 1998, pg 209-212.

Millitech, 2004, *Overview of Calculating System Minimum Detectable Signal*, LLC • 29 Industrial Drive East, Northampton, MA 01060 USA, p. 1

Mutlu, S., 1997, *Surface Micromachined Capacitive Accelerometer With Closed-Loop Feedback*, Ann Arbor, Michigan 48109-2122, p. 4

Oosterbroek, Ir. R.E. (1999, November 12), "Modeling, design and realization of microfluidic components", Ph.D. thesis University of Twente, ISBN 90-36513464.

PC-CONTROL. Pc-control [online]. Available from:

<http://www.pc-control.co.uk>

PCMAG-ENCYCLOPEDIA. Pcmag-Encyclopedia [online]. Available from:

http://www.pcmag.com/encyclopedia_term/0,2542,t=accelerometer&i=37372,00.asp

Petersen, K., "Silicon as a mechanical material", *Proc. IEEE*, Vol-70, 1982, pp 420-457.

PRODUCT OF ANALOG. Product of Analog [online]. Available from:

<http://www.analog.com/en/subCat/0,2879,764%255F800%255F0%255F0%255F0%255F0%255F0,00.html>

Qing-Ming Wang, Zhaochun Yang, Fang Li, Patrick Smolinski, Analysis of thin film piezoelectric microaccelerometer using analytical and finite element modeling, *Sensors and Actuators A* 113 (2004) 1–11, p. 5

Schwingungsmesstechnik [online]. Available from:

<http://www.mmf.de>

SENSORSMAG. Sensorsmag [online]. Available from:

http://www.sensorsmag.com/articles/0399/0399_44/main.shtml

Stein, J., 1995a, Microelectronic acceleration sensors, Proceedings of the 4th Intl. Workshop "Measurement '95", p. 44

Stein, J., 1995b, New trends in acceleration sensors, *Automatizace* 38, pp.175-177

Wiegerink, R.J., Zijze, A.F., Krijnen, G.J.M., Lammerink, T.S.J., & Elwenspoek, M.C. (1999, January 17). Quasi monolithic silicon load cell for loads up to 1000 kg with insensitivity to non-homogenous load distributions, [Proceedings, MEMS'99 Conference]. (pp. 558-563). Orlando, USA. ISBN 0-7803-5194-0.

Yazdi, N., Ayzi, F., and Najafi, K., Micromachined inertial sensors, *Proc. IEEE*, Vol-86, 1998, pp. 1640-1659.

Resume of Fei GUO

Name: Fei GUO

Birth: December 24, 1979

Gender: Male

Degree: B.Sc. (Beijing Union University, China, 2002)

Current Situation: Studying for Master Degree of Technology (Cape Peninsula University of Technology, South Africa)

Research interests: Design and Analysis of Micro Accelerometers